# Fast and partitioned postglacial rebound of southwestern Iceland

Guillaume Biessy, Olivier Dauteuil, Brigitte van Vliet-Lanoë, A. Wayolle

# Fast and partitioned postglacial rebound of southwestern Iceland

G. Biessy,[1] O. Dauteuil,[1] B. Van Vliet-Lanoë,[2] and A. Wayolle[2]

Received 24 June 2007; revised 11 January 2008; accepted 15 February 2008; published 9 May 2008.

[1] Located both on the Mid-Atlantic Ridge and above a mantle plume, Iceland is subject to horizontal and vertical motions. Many studies described these deformations in terms of rifting episodes that have combined both extensional tectonics and magmatism. However, few studies have described the glacio-isostatic response induced by the retreat of the Weichselian ice cap. The melting of this ice cap induced a postglacial rebound for the whole of Iceland that may be controlled by the geodynamic setting and the rheological layering of the lithosphere. This study is devoted to (1) understanding the Holocene rebound on the southwestern coast and (2) estimating the asthenosphere viscosity and depth beneath Iceland. Two stages of holocene evolution were determined by means of GPS profiles, morphological observations, and data compilation. The first stage corresponds to a vertical uplift of 67.5 to 157.5 m. It started at 10,000 years BP and ended at 8500 years BP implying uplift rates between 4.5 and 10.5 cm/a. It was a quick isostatic response to the fast ice retreat. The second stage had vertical motion of tens of meters with a probable tectonic origin and started at 8500 years BP. The uplift rate is 1 to 2 orders of magnitude slower than the one during the first stage. Uplift partitioning during the first stage was controlled by the thermal state of the lithosphere, the highest geothermal flux inducing the maximum uplift rates. The relaxation time for uplift provides a viscosity estimate of 5.4–5.8 $\times$ $10^{19}$ Pa s for the asthenosphere. This value is similar to those determined for glacial areas in different continental contexts. However, the flexural wavelength indicates a shallower asthenosphere than that occurring in continental domains. Therefore this study highlights a coupling between the thermal structure of the Icelandic asthenosphere and the glacial rebound. **Citation:** Biessy, G., O. Dauteuil, B. Van Vliet-Lanoë, and A. Wayolle (2008), Fast and partitioned postglacial rebound of southwestern Iceland, *Tectonics*, *27*, TC3002, doi:10.1029/2007TC002177.

## 1. Introduction

[2] In Iceland, the conjunction of the Mid-Atlantic Ridge and a mantle plume creates intense tectonic and magmatic activities. These combined processes lead to deformation with large horizontal and vertical components. Horizontal motions are mainly induced by the divergence between the North American and European plates, trending at N110°E with a half spreading rate of 0.9 cm/a [*DeMets et al.*, 1994]. However, single rifting events generate higher strain rates that may reach tens of centimeters to meters per year [*Gudmundsson et al.*, 1999; *Zobin*, 1999; *Dauteuil et al.*, 2001; *Bellou et al.*, 2005]. Whereas the origin of the horizontal motions is well established, vertical motions result from multiple processes [*Dauteuil et al.*, 2005], such as glacio-isostasy, regional tilting, transform zones, hot spot doming, deep intrusion or volcanism. Each process has its own characteristic wavelength (meters to hundreds of kilometers), rate (mm/a to m/a) and displacement amount (cm to hundreds of meters). The present analysis on the postglacial rebound, which occurred after the retreat of the last Weichselian ice cap on Iceland, was the major aim of this study. This rebound was poorly studied because it was assumed to have a small vertical component compared to the tectonic and magmatic processes.

[3] The Icelandic plateau underwent several glaciations during the Quaternary. According to *Einarsson and Albertsson* [1988], 15–23 glaciations affected Iceland during the past three million years, including the last one, the Weichselian glaciation ended at 9000 years BP. During a glacial stage, the ice sheet increases the vertical loading of the lithosphere and leads to a subsidence of the bedrock surface, controlled by both the lithosphere elasticity and the asthenosphere viscosity [*Stewart et al.*, 2000]. A rough estimate shows that the island subsides 300 m under an ice sheet 1000 m thick. During the deglaciation, the retreat of the ice cap unloads the basement and induces an uplift of Iceland with a complex pattern: the quick decrease of the vertical stresses generates an elastic rebound with basement uplift, faulting and seismicity. In such a context, the horizontal stresses are gradually relaxed by the viscoelastic return flow of the mantle material [*Stewart et al.*, 2000]. Furthermore, the high geothermal gradient due to the geodynamic pattern of Iceland induces a thin lithosphere [*Bourgeois*, 2000] and a mantle viscosity at shallow depths that is smaller than in a normal continental context. This raises a question: does the specific Icelandic context emphasize the glacial rebound? While horizontal deformation has been widely studied in

[1] Géosciences Rennes, UMR 6118 CNRS, Université de Rennes 1, Rennes, France.
[2] Processus et Bilan des Domaines Sédimentaires, UMR 8110 CNRS, Université de Lille 1, Villeneuve d'Ascq, France.


0278-7407/08/2007TC002177

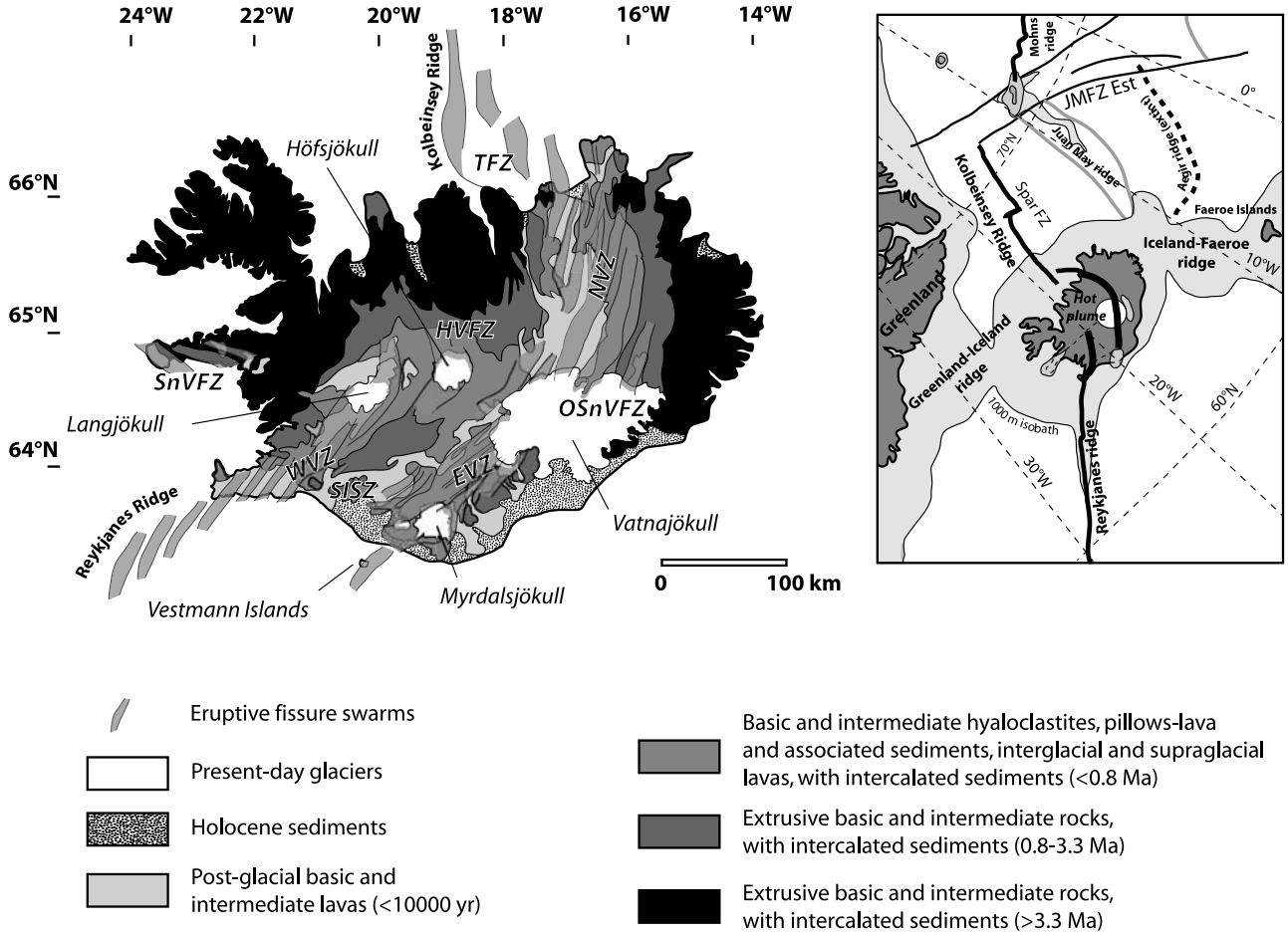


**Figure 1.** Geological setting of Iceland [*Johannesson and Saemundsson*, 1998]. Iceland lies at the junction between the Reykjanes Ridge in the southwest, the Kolbeinsey Ridge in the north, and a hot spot, whose apex is located under the Vatnajökull ice cap. Current tectono-volcanic activity occurs in the Neovolcanic Zone, composed of three main segments, the Northern (NVZ), Western (WVZ), and Eastern (EVZ) Volcanic Zones. The Snaefellsjökull peninsula (SnVFZ), Höfsjökull (HFVZ) and Öraefajökull-Snaefell (OSnVFZ) flanck zones are also active. SISZ, South Iceland Seismic Zone; TFZ, Tjörnes Fracture Zone.

Iceland, the vertical motions were not so intensively studied. The purpose of this paper is to determine uplift rates on the southwestern coast of Iceland and its spatial variations. To determine the rebound pattern, we focused on (1) field work based on a detailed mapping of coastal surfaces with high-resolution GPS, (2) analysis of geological and geomorphologic data, and (3) estimate of vertical motions including eustatic variations since the Last Glacial Maximum. These uplift rates allowed us to determine a mean viscosity for the Icelandic asthenosphere.

## 2. Geological Setting

### 2.1. Geodynamic Framework

[4] The Iceland Plateau and the Greenland-Faeroe Ridge are conspicuous bathymetric features in the NE Atlantic Ocean (Figure 1). These shallow areas have an anomalously thick oceanic crust resulting from a high magmatic supply due to the plume [*Kaban et al.*, 2002]. In Iceland, there is a consensus that crustal thickness varies from about 40 km under Vatnajökull to less than 20 km under the northern part of the North Volcanic Zone and the Reykjanes Peninsula [*Menke et al.*, 1998; *Darbyshire et al.*, 2000; *Kaban et al.*, 2002; *Foulger et al.*, 2003]. The extensional processes are controlled by rift jumps that are largely emphasized by magma supply [*Helgason*, 1984, 1985; *Garcia et al.*, 2003] and a succession of volcanic roll-overs [*Bourgeois et al.*, 2005].

[5] The build-up of the Icelandic plateau began 25 Ma ago. The present direction of divergence between the North American and Eurasian plates is N110°E with a half spreading rate of 0.9 cm/a [*DeMets et al.*, 1994]. Nowadays the crustal accretion connecting the ridges of Reykjanes and Kolbeinsey crosses Iceland from the southwest to the north inside the Neovolcanic Zone. This area covered by interglacial to subglacial volcanic formations younger than

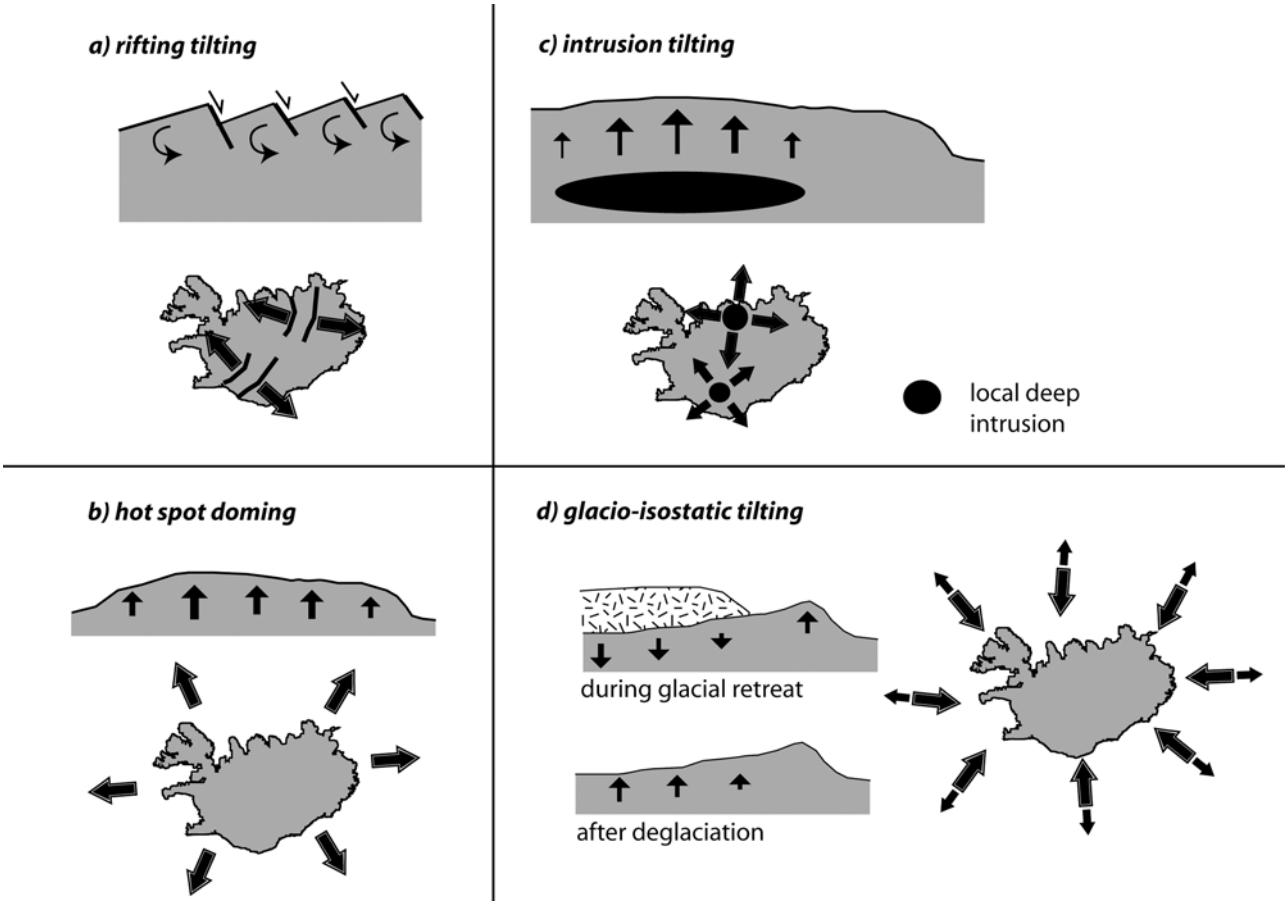


**Figure 2.** Models of processes generating vertical motions in Iceland (modified from *Dauteuil et al.* [2005]). See text for further explanations.

800 ka is subdivided into three rift systems: the Western Volcanic Zone (WVZ) that extends from the Reykjanes peninsula to the Langjökull glacier, the Eastern Volcanic Zone (EVZ) from the Vestmann Islands to the Vatnajökull glacier, and the Northern Volcanic Zone (NVZ) from the Vatnajökull glacier to the northern coast of Iceland (Figure 1). The external zone located on both sides of the Neovolcanic Zone is made up of basalt lava flows emplaced from 16 Ma to 800 ka [*Saemundsson*, 1978, 1979].

[6] The shape of the Icelandic plateau results from lava accumulation, erosion and depositional processes. Two large-scale erosion surfaces shape the island: the 600- to 700-m-high inland plateau and the coastal area whose elevation ranges from +100 m to −400 m. Successive ice sheets shaped the upper surface that is topped by Holocene volcanism and recent erosion. The coastal morphology displays various patterns: large areas of fjords in the northwest and the southeast of the island, flat alluvial to proglacial plains (sandurs) and tidal erosion surfaces (strandflats) in the south and the west. The elevation of the coastal zone reaches 80–90 m, as far as 50 km onshore from the shore. However, it is largely submerged, until a depth of 100 m. In the sandur area, wide depositional plains have been regularly retrimmed by catastrophic floods and result from subglacial volcanic eruptions or ruptured ice-dammed lakes (jokülhlaup). Thus, they are located downstream of ice caps, often in the vicinity of an active volcanic zone. A strandflat is a coastal platform common to mid to high latitudes and of variable extent [*Van Vliet-Lanoë*, 2005]. These surfaces are quite extensive along the northern Atlantic [*Guilcher et al.*, 1994]. The processes responsible for their formation are still debated: marine abrasion, glacial or periglacial erosion, continental erosion, tectonic platform, etc. The most probable hypothesis is a Mio-Pliocene tidal abrasion platform, partly retrimmed by glacial dynamics during the Quaternary [*Van Vliet-Lanoë*, 2005]. Indeed these surfaces often display "roche moutonnée" or block quarrying features.

### 2.2. Vertical Motion Balance

[7] Various dynamic processes generate vertical motions in Iceland. They lead to either large-scale deformation of the whole island, or local effects [*Dauteuil et al.*, 2005] (Figure 2).

[8] 1. Rifting and spreading processes generate either tilted blocks distributed in a large area or a large-scale flexure, as on passive margins or in continental rifts [*Braun and Beaumont*, 1989; *Chéry et al.*, 1992; *Hopper and Buck*, 1998] (Figure 2a). In Iceland, deformation due to spreading

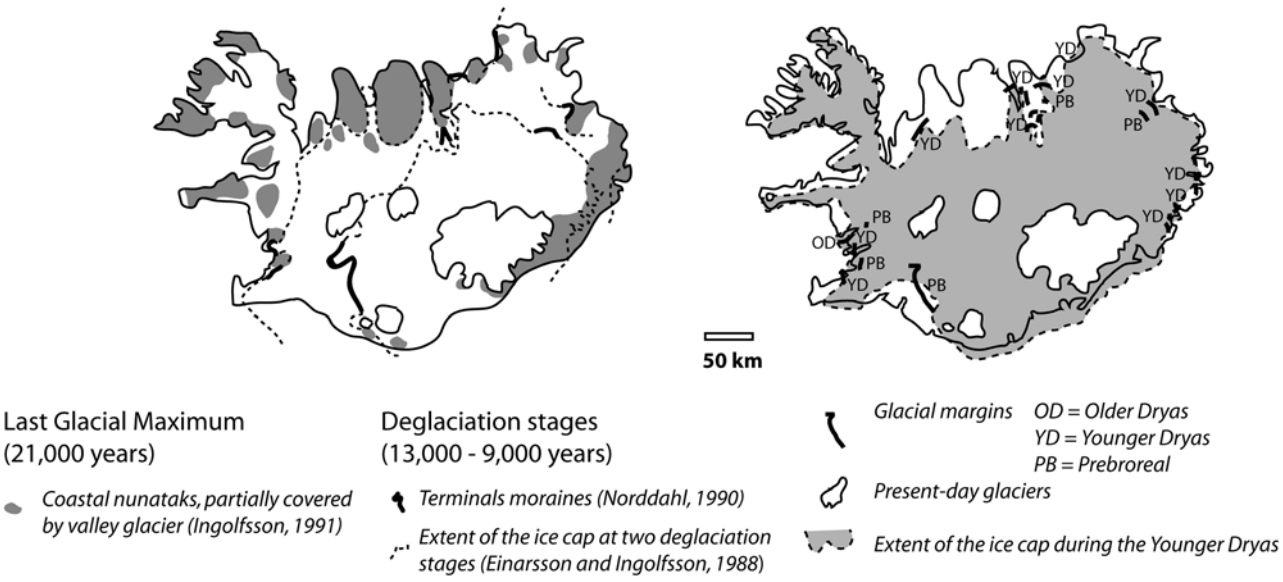


**Figure 3.** Extent of the Weichselian ice cap on Iceland at different periods (modified from *Bourgeois* [2000]) and at the Younger Dryas (modified from *Ingolfsson et al.* [1997]).

produces successive roll-overs that migrate to accommodate the absolute westward displacement of the North Atlantic plate relative to the Icelandic hot spot [*Helgason*, 1984, 1985; *Garcia et al.*, 2003; *Bourgeois et al.*, 2005]. Basaltic lava flows dip toward the active rift zone: this tilting is controlled by a main normal listric fault, generally located on the westward side of the roll-overs. This pattern leads to asymmetric vertical motion with high and localized deformation above the main listric fault and gentle flexure and widespread fissuring on the opposite side. This deformation occurs inside the active rift. A few papers have described vertical displacement outside the active zone. *Hofton and Foulger* [1996a, 1996b] and *Dauteuil et al.* [2005] estimate significant rate (1–2 cm/a) on both side of the northern rift. Their origin remains debated and rifting processes are suggested.

[9] 2. A thermal bulge and a dynamic topography created by the ascending mantle plume lead to vertical displacements (Figure 2b). The uplift maximum is located above the center of the hot spot and produces dome topography. The 1000-m uplifts with wavelengths of several hundreds of kilometers have been described [*Sheth*, 1999; *Lundin and Doré*, 2002]. This large-scale doming can be observed on the bathymetric map of the North Atlantic Ocean that displays abnormal shallow depths from the Charlie-Gibbs Transform Zone in the south to Mohns Ridge in the north. In these contexts, a tilt of less than 1° affects the lava flows. They are tilted outward from the center of the hot spot.

[10] 3. The magmatic dynamics inside the crust creates rapid and localized vertical motions. They are induced both by the magma supply before and during eruption and by the withdrawal of the magmatic reservoir after the eruption (Figure 2c). The interferometric techniques map perfectly this deformation [*Henriot et al.*, 2001; *Clifton et al.*, 2002]. Some studies realized on the Krafla volcanic system revealed that the deflation consecutive to the last main eruption goes on more than 20 years after the event and affects an elongated area with an average rate of 2 cm/a [*Henriot et al.*, 2001].

[11] 4. Glacio-isostatic adjustments induced large-scale to local vertical displacements (Figure 2d). The overload associated to the emplacement of an ice cap leads to a progressive sinking of the crust called glacio-isostatic deformation. This flexure is slow in a context of thick and rigid lithosphere, as in the Canadian and Scandinavian shields, and faster in a context of thin and hot lithosphere, such as in Iceland. The amplitude of the deformation may reach 900 m in Iceland [*Van Vliet-Lanoë*, 2005]. During a deglaciation stage, the ice sheet thins up first on the coast and then the glacial retreat migrates inland. Thus, the loading/unloading effect is larger and quicker close to the coast than in the island center. This creates a differential uplift between the coast and the inland zone, generating an apparent tilting toward the internal zone of shoreline features [*Dauteuil et al.*, 2005]. In this study, we aimed to determine vertical motions created by glacio-isostasy, after the retreat of the Weichselian ice cap at 10,000 years BP, using displacements of shorelines and eustatic variations.

### 2.3. Weichselian Ice Cap

[12] In Iceland, the Weichselian glaciation started after the Eemian period, at 130,000–110,000 years BP [*Einarsson and Albertsson*, 1988; *Norddahl*, 1990; *Van Vliet-Lanoë et al.*, 2001; *Van Vliet-Lanoë*, 2005]. Glacial extents during the coldest period of the Last Glacial Maximum (LGM) and at the Younger Dryas (11,000–10,000 years BP) are controversial (Figure 3). Some authors have argued for an ice sheet reaching the outer edge of the island shelf [*Hoppe*,

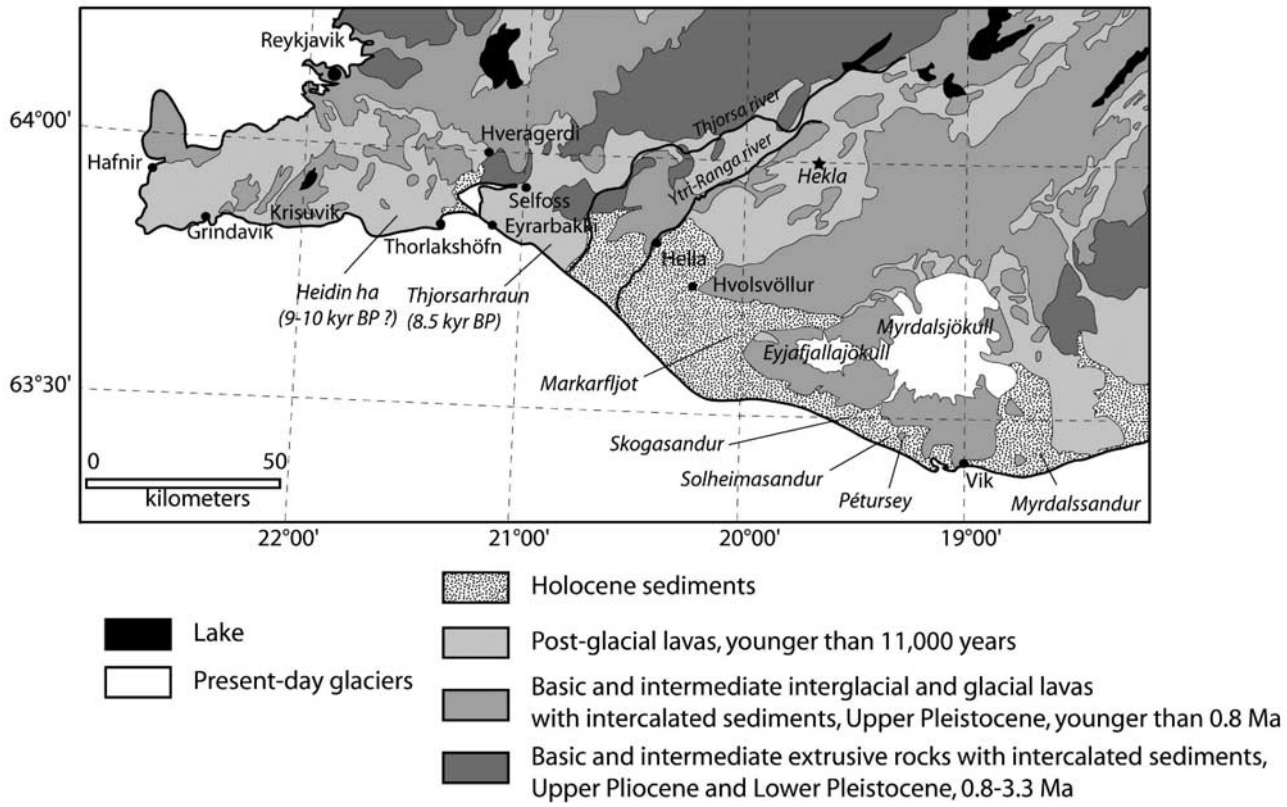


**Figure 4.** Geological map of the southwestern coast of Iceland.

1982; *Norddahl and Halfidason*, 1992; *Ingolfsson and Norddahl*, 2001]. Recent inland geological observations supported by dating in the south and in the northwest shelves imply a more limited extent at the LGM and at the Younger Dryas [*Geirsdottir et al.*, 1997; *Andrews et al.*, 2000; *Andrews and Helgadottir*, 2003]. These data confirm earlier observations of a limited ice sheet [*Einarsson and Albertsson*, 1988; *Ingolfsson*, 1991]. The analysis of ice cores provides a maximum of aridity at 25,000 years BP (NGRIP Project [*Mortensen et al.*, 2005]). The record in the loess of occidental Europe indicates that it occurred between to 25,000 to 17,000 years BP [*Van Vliet-Lanoë*, 2005]. The lowest sea level is recorded from 26,000 to 20,000 years BP [*Peltier and Fairbanks*, 2006].

[13] A limited deglaciation, argued on undated terminal moraines close to the present shores, is generally considered to represent the Younger Dryas or even the Preboreal extent [*Norddahl and Halfidason*, 1992; *Ingolfsson et al.*, 1997; *Ingolfsson and Norddahl*, 2001]. Classically the deglaciation in Iceland is considered to set in from 13,000 years BP [*Norddahl*, 1990; *Ingolfsson*, 1991; *Ingolfsson and Norddahl*, 1994; *Ingolfsson et al.*, 1997] with several stages of ice advance and retreat. There were two major advances of similar extent at 15,000 years BP and during the Younger Dryas in the close vicinity of the present shoreline.

[14] On the basis of the maximal extent of the LGM ice cap and the corresponding theoretical dynamic profile, *Jull and McKenzie* [1996] estimated an ice thickness of about 2000 m in the center of Iceland. This value is incompatible with the thickness determined from elevations of the highest erosional features or of glacial deposits on coastal relieves, and from the elevation of subglacial volcanoes in the center of the island [*Einarsson and Albertsson*, 1988; *Norddahl*, 1990, 1991]. These studies showed that the ice thickness was maximal in the Vatnajökull area (1000 to 1500 m), decreased toward the north and the west, and reached 300 to 500 m along the current coastline.

### 2.4. Study Area

[15] This study is focused on the southwest Iceland from the Reykjanes peninsula to Vik town where several dated Holocene markers such as lava flows, glacio-marine transgressive deposits dated by radiocarbon and large Holocene sandurs can be observed (Figure 4). The limited vegetation on the Reykjanes peninsula allows optimal observations of the outcrops. The volcanic system of Reykjanes consists of four NE-SW en-echelon ridges crossing the peninsula. They are composed of subglacial structures, as móberg ridges and table mountains, and submarine volcanic structures, topped by Holocene aerial lava flows. The central part of the study area extends from Hveragerdi in the west to Hvolsvöllur in the east. It includes the main EW transfer zone linking the Western (WVZ) and Eastern Volcanic Zones (EVZ) with intense seismic activity (SISZ). The topography of the area is very contrasted with low coastal plains in the south, covered either by post-glacial lava flows in the west

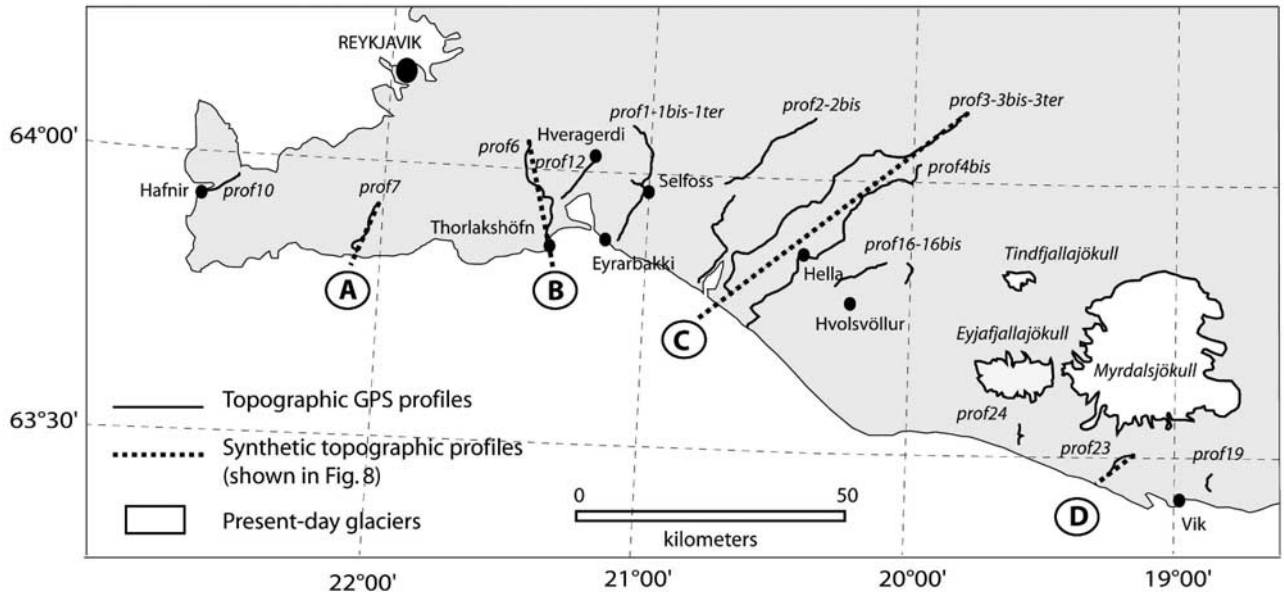


**Figure 5.** Location of the topographic GPS profiles (1–23) and of the synthetic profiles (A–D) used in this study. The synthetic profiles were presented in Figure 8, which illustrates the main results and allowed drawing the map of Figure 9.

(Thjorsarhraun lava) or by Holocene fluvioglacial sediments (sandurs) in the east. Higher mountains (1000–1500 m) are formed by Upper Pliocene-Lower Pleistocene flows, hyaloclastite ridges and postglacial lava flows from the fissures vents of Hekla volcano. The eastern part of the study area extends from the Márkarfljót River in the west to Vik town in the east. This area is characterized by large Holocene fluvioglacial plains from the present-day shoreline to the high marine cliffs formed by hyaloclastites and interglacial lavas [*Thordarson and Hoskuldsson*, 2002]. As the LGM ice cap extent is poorly constrained, we have limited our work to the South Western Rift Zone, where the Younger Dryas and Preboreal terminal moraines are fairly preserved.

## 3. Methodology

### 3.1. Topographic Profiles

[16] The first step was to recognize the different geomorphologic markers corresponding to sea levels and ice locations. To map topographic profiles across the coastal plain, we used GPS, with post-processing differential corrections. This method needs two receivers: one for the rover mapping and another one used as a fixed reference GPS station. During the work, we used three receivers: a monofrequency 4600 LS model for the reference station and two PROXRS for the mapping, both manufactured by TRIMBLE. The reference station was daily installed on a tripod at the center of the study area. We postprocessed the data with Pathfinder Office software developed by TRIMBLE. After the differential postprocessing, these monofrequency receivers provided a horizontal accuracy of 0.5–1 m and a vertical accuracy of 1 m, depending on the profile. This accuracy is sufficient for mapping features such as past marine cliffs, moraine ramparts and deposit/erosion surfaces. We measured about 375 km of topographic data along 35 profiles on the southwestern coast of Iceland. Most of them were done from the present shoreline to the interior of the island, perpendicularly to the coast, until the first cliff limiting the glacial and marine abrasion surfaces or the transition between glacio-marine and fluvioglacial facies.

[17] Twelve synthetic profiles representative of field observations were built to determine the Holocene evolution (Figure 5). For each initial raw profile, we defined a mean azimuth and we projected topographic data onto the new synthetic profile. Onto these synthetic profiles we draped geological and geomorphologic data issue from a 1/500,000 geological map [*Johannesson and Saemundsson*, 1998] and from our observations.

### 3.2. Method of Uplift Estimation

[18] We combined the elevations of geological markers belonging to past marine cliffs with eustatic variations known since the LGM to determine uplift amounts in southwestern Iceland (Figures 6a and 6b). We used the classical method of recorded shoreline displacement [*Ingolfsson et al.*, 1995]. At $t = t_1$, the relative sea level (RSL) is at $z = z_1$ below the present-day sea level. The RSL variation between the elevation $z_1$ at $t_1$ and the elevation $z_2$ at $t_2$ (more ancient than $t_1$) is: $\Delta z(RSL)_{21} = z_1 - z_2 > 0$ because of the rising of the sea level. To determine the absolute amount of uplift or subsidence of Iceland, we must add the elevation difference, at $t = t_1$, between the former marine marker (F1) and the new one ($F_1''$): $\delta z_{21} = z_{F1} - z_{F''1}$. Consequently, we obtain: $\Delta z(\text{Iceland})_{21} = \Delta z(RSL)_{21} +$

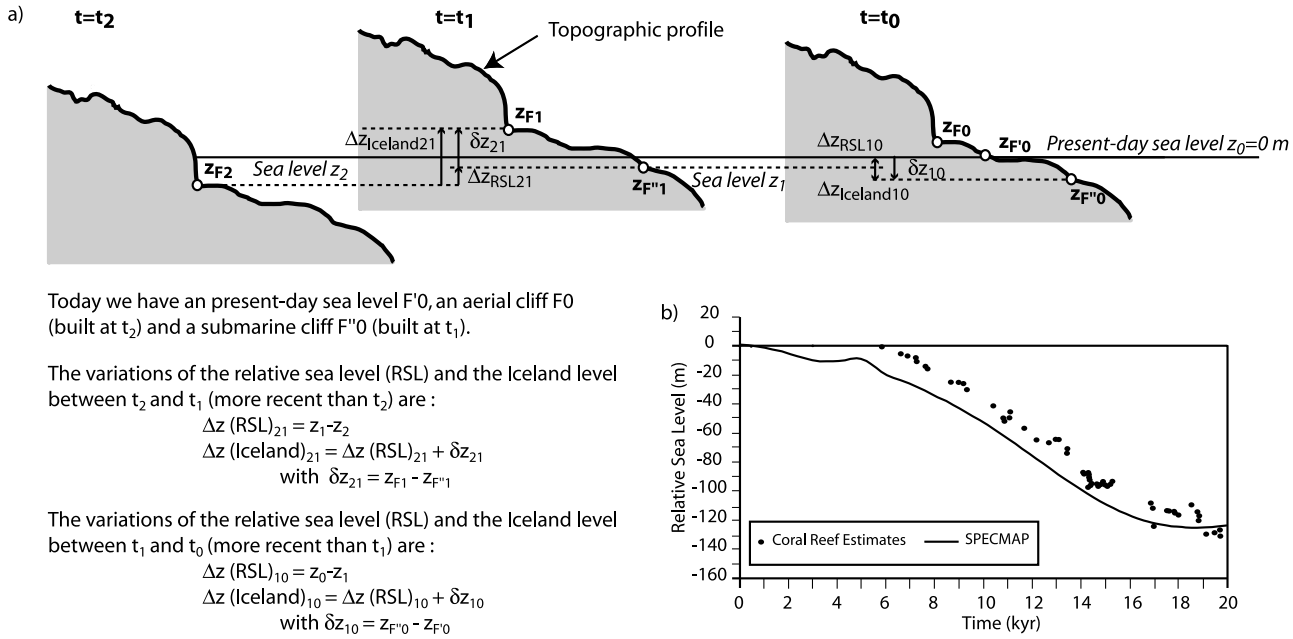


**Figure 6.** (a) Estimation of uplift integrating eustatic variations. See text for further explanations. (b) Eustatic curves since the Last Glacial Maximum as compared to the present-day sea level [*Jouet*, 2003; *Jouet et al.*, 2006]. Note the gap of 15–20 m between the two curves Coral Reef and SPECMAP.

$\delta z_{21}$. There are three possibilities: (1) if $\delta z_{21} > 0$, so $\Delta z(\text{Iceland})_{21} > \Delta z(\text{RSL})_{21} > 0$ and so Iceland rises faster than relative sea level; (2) if $\delta z_{21} < 0$ and $|\delta z_{21}| < |\Delta z(\text{RSL})_{21}|$, so $\Delta z(\text{RSL})_{21} > \Delta z(\text{Iceland})_{21} > 0$ and so Iceland rises more slowly than relative sea level; and (3) if $\delta z_{21} < 0$ and $|\delta z_{21}| > |\Delta z(\text{RSL})_{21}|$, so $\Delta z(\text{Iceland})_{21} < 0$, so that Iceland subsides.

[19] At $t = t_0$, the RSL is at the present sea level. The RSL variation between the elevation $z_0$ at $t_0$ and the one $z_1$at $t_1$ (more ancient than $t_0$) is: $\Delta z(\text{RSL})_{10} = z_0 - z_1 > 0$ because of the rising of the sea level. To determine the amount of uplift or subsidence, we must add the elevation difference, at $t = t_0$, between the former marine marker ($F_0''$) and the new one ($F_0'$): $\delta z_{10} = z_{F''0} - z_{F'0}$. Consequently, we obtained for Iceland: $\Delta z(\text{Iceland})_{10} = \Delta z(\text{RSL})_{10} + \delta z_{10}$ and the same three possibilities exist.

[20] The eustatic variations since the LGM are given by two curves, Coral Reef curve and SPECMAP curve [*Jouet*, 2003; *Jouet et al.*, 2006] (Figure 6b). The Coral Reef curve is based on a compilation of measurements done on reef-building corals of the Pacific Ocean dated with Uranium-Thorium-Lead age method. The SPECMAP curve is based on forams determined from deep-sea sediment cores, with different cores merged to one synthetic curve. These two curves show that the sea level was 120 m below the present-day one at the LGM with little changes until 16,000 years BP, after which it began to rise progressively (~1 cm/a). At 6,000 years BP, the sea level is the same as today for the Coral Reef estimation, whereas it is rising more slowly for the SPECMAP model (0.3 cm/a). The water melt pulses may explain the delay of 15–20 m in sea level rise between the two curves occurring 16 ka BP ago [*Peltier*, 2005; *Peltier and Fairbanks*, 2006].

## 4. Results

### 4.1. Geological and Geomorphologic Observations

[21] Markers of glacial extent, ancient marine shorelines, fluvioglacial drift plains, marine or glacial erosion surface, marine cliffs and terminal moraines were recorded to determine the Holocene evolution of shorelines. The age of the different markers was constrained by using both Holocene lava flows and complementary data, such as tephra and marine fossils.

[22] Marine cliffs limit the coastal plains along the southwestern coast of Iceland. These cliffs display sharp basal notches, fresh scarps and unsmoothed top edges in the Reykjanes peninsula and around Vik (Figure 7a). The upper surfaces were shaped by glacial erosion. The scarps are important in these two zones: 150 m for the Reykjanes peninsula and 300–350 m for Vik. Gravels of paleo-beaches covered flat tidal surfaces in the Reykjanes peninsula. Paleo-beaches could be observed around Hveragerdi (Figure 7b) and in the western Reykjanes peninsula. These surfaces are roughly flat, covered by rounded marine pebbles and shingles - lying sometimes on flat tidal abrasion surfaces or retrimming fans. They were used as the boundary between land and sea when sea level was estimated to be relatively higher. In Vik area, they are buried by prograding sandurs (Figure 7a). Another type of marine cliff was observed in the central part of the study area. This last type corresponds to small scarps (20–25 m) built up either in an

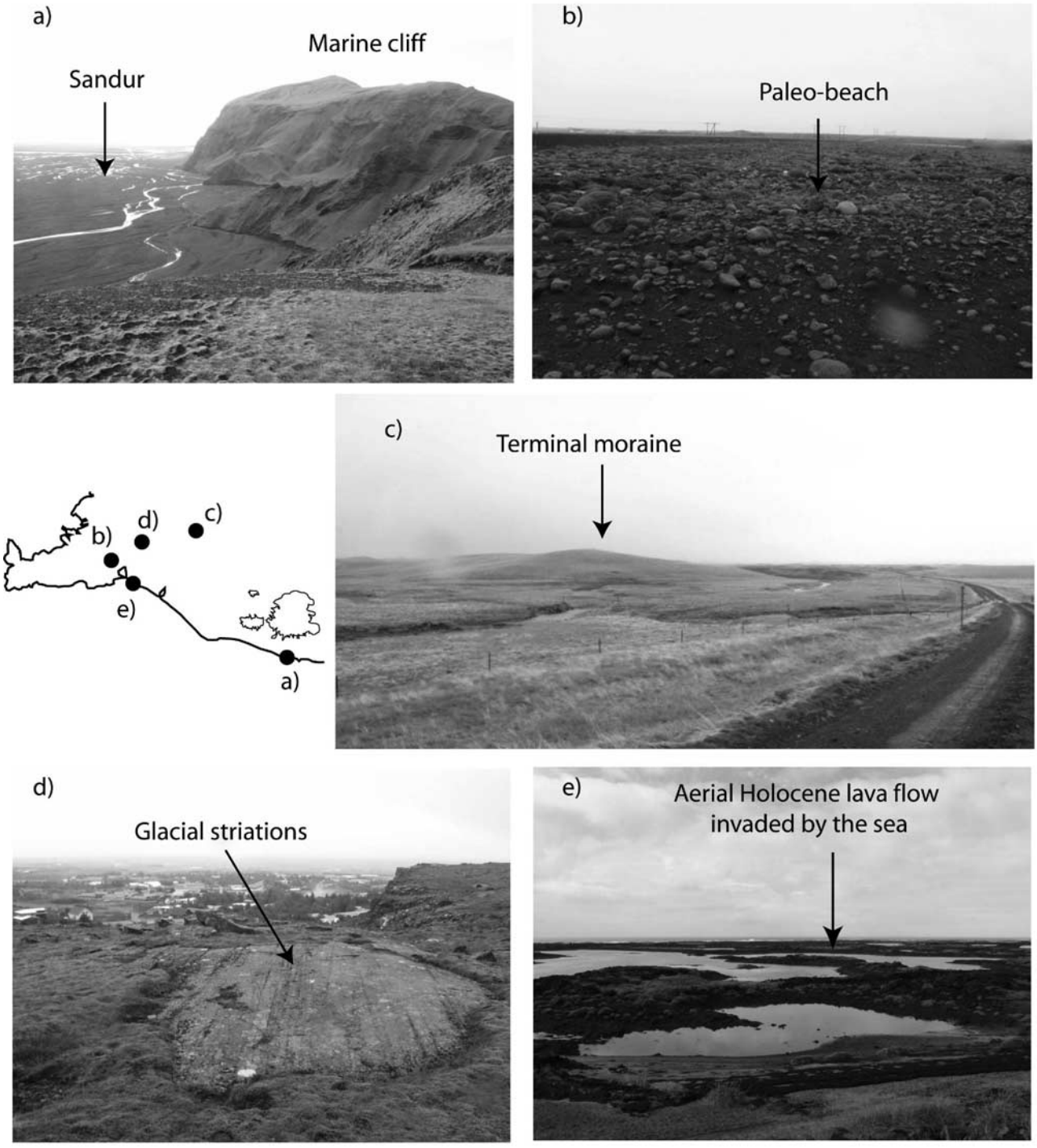


**Figure 7.** Different geological and geomorphologic markers observed along the southwestern coast. (a) Marine cliff with a fluvioglacial drift plain (sandur) near Vik. (b) Paleo-beach in the south of Hveragerdi at the base of a cliff. (c) Terminal moraine of the Budi system in the north of Hella. (d) Glacial striations on interglacial basalt, Hveragerdi. (e) Aerial Holocene lava flow invaded by the sea level off Eyrarbakki. (Pictures courtesy of G. Biessy.)

interglacial or supraglacial lavas (<0.8 Ma) or in extrusive rocks (0.8–3.3 Ma) [*Johannesson and Saemundsson*, 1998].

[23] Some discontinuous systems of terminal moraines (Figure 7c) show the last stage of glacier readvances north of Hella town. These moraines belong to the moraine system of Budi, a set of 20- to 25-m-high hills across the southern plains. This moraine system was built during the Younger Dryas extension (11–10 ka BP), with a retreat position of the glacier at the Preboreal (10–9.3 ka BP) [*Geirsdottir et al.*, 1997].

[24] Glacial striations (Figure 7d) appear on interglacial lavas flows older than 110–130 ka BP in the area of Hveragerdi [*Johannesson and Saemundsson*, 1998]. These striations are fine grooves incised in the basement by materials embedded at the base of the mobile ice. We observed postglacial lava flows invaded by the present sea level in the Reykjanes peninsula (areas of Thorlakshöfn and Hafnir, Figure 7e) and breaking off waves indicating abrupt slope break. The Holocene lavas flowed in subaerial conditions during a low marine stand, which probably created a marine notch responsible for breaking waves located away from the present-day shoreline. Then the global rise of the sea level drowned these aerial lava flows. The ages of the early aerial lava flows thus provide critical constrains on the age and the location of the marine low-stands.

### 4.2. Geological Sections

[25] Four synthetic sections were drawn, on the basis of topographic profiles, geologic data and geomorphologic observations (Figure 8). They trend perpendicular to the present-day coastline and will be described from west to east.

[26] Sections A and B were surveyed in the center and east of the Reykjanes peninsula, respectively. In Krisuvik area, section A crosses an interglacial lava field and hyaloclastite formations (Figure 8a). At the southern end of the profile, a 25-m-high former marine cliff constrains the extent of marine deposits, a paleo-beach surface at an elevation of +50 m. North to this marine marker, the profile displays a glacial abrasion surface at an elevation of +90–100 m.

[27] Section B crosses the Heidin Há lava flow, from north of Hveragerdi to Thorlakshöfn on the coast (Figure 8b). This section is characterized by a 125-m-high marine cliff. At its base, the tidal flat is at an elevation of +56 m and the associated notch is partly buried under postglacial lava flows. At the northern end of the profile (prof12; see Figure 5 for location), a raised tidal flat covered by cobbles at the base of the cliff is at 50-m elevation. A lava flow probably also covered this surface on profile B. Furthermore, this postglacial lava flow is today drowned by the present-day sea level, near Thorlakshöfn. It formed subaerially, during a low stage of the sea, and then was drowned during a rise of relative sea level. The southernmost extent of the profile B displays a clear knickpoint located offshore at a 40-m depth which appears to occur all around the Reykjanes peninsula. This submerged cliff causes breaking waves off Hafnir and Keflavik. Consequently, the Reykjanes peninsula displays two former marine levels at present-day elevations of +50 to 55 m and −40 m, and a maximum extent of the ice cap at the top of the cliffs, at more than +90 m. Marine deposits on the peninsula, dated at 21 ka and 12 ka BP [*Norddahl and Pétursson*, 2005], provide evidence for early deglaciation of the peninsula, prior to the Younger Dryas.

[28] Section C sums up three profiles measured along the Thjorsa River between Selfoss and Hella (Figure 8c). From south to north, it crosses a sandur, interglacial lavas, late glacial lavas and postglacial lava flows of Thjorsarhraun (8.5 ka BP) and Tungnaahraun (6.7 ka BP) [*Thordarson and Hoskuldsson*, 2002]. A 20-m-high former marine cliff with Holocene sandur has a base at an elevation of +10 m. This marine notch is also recorded on the two lateral profiles (prof2–2bis and prof4–4bis; see Figure 5) on both sides of profile C. We observed two 25- to 30-m-high terminal moraines of the Budi moraine system northward [*Geirsdottir et al.*, 1997]. The extent of the ice cap is at an elevation of +80 to 90 m. In this region, the average thickness of the sandur is 10 to 15 m. It commonly lies on late interglacial alluvia and older terminal moraines, except along the Thjorsa River where it has been regularly and deeply buried by early and middle Holocene jokülhlaups.

[29] Section D is west of Vik, through the large sandur of Solheimasandur (Figure 8d) near mount Pétursey. The latter mount is an isolated scarped hill, a relic of a submarine emergent volcano formed when the flat coastal plains were totally submerged by the sea [*Thordarson and Hoskuldsson*, 2002]. The present-day position of the shoreline and the important volume of sediment carried by active glacial outlet rivers allow the isolation of these former islands. Section D has a typical shape of the profiles observed in this area, with its marine cliff at an elevation of more than 300 m and sandur deposits with a gentle slope from its base to the present-day shoreline. The thickness of fluvioglacial sandur is unknown. From studies on Skeidarársandur, in the southwest of the Vatnajökull ice cap, the thickness is 70–80 m in the north of the alluvial plain and 200 to 250 m near the present-day shoreline [*Gudmundsson et al.*, 2002]. The ice volume and the present-day glacial rivers are smaller in the Solheimasandur area, implying that thinner sandur is expected. The elevation of the marine level is variable on the west coast of Vik (15, 38 and 75 m) because of the occurrence of these sediments. It is impossible to determine the vertical location of the marine cliff base. Additional work was done in this area with electrical tomography. Two profiles were measured, one at the base on the present-day cliff and a second one on the sandur. The electric investi-

**Figure 8.** Geological synthetic sections combining GPS profiles, field observations and previous works. (a) Section A at Krisuvik. (b) Section B from Hveragerdi to Thorlakshöfn. (c) Section C, along the left bank of the Thjorsa river. (d) Section D, west of Vik, near Pétursey (the cliff of Alftagrof was added to the topographic profile). All profiles are plotted with vertical exaggeration. They are located on Figure 5.

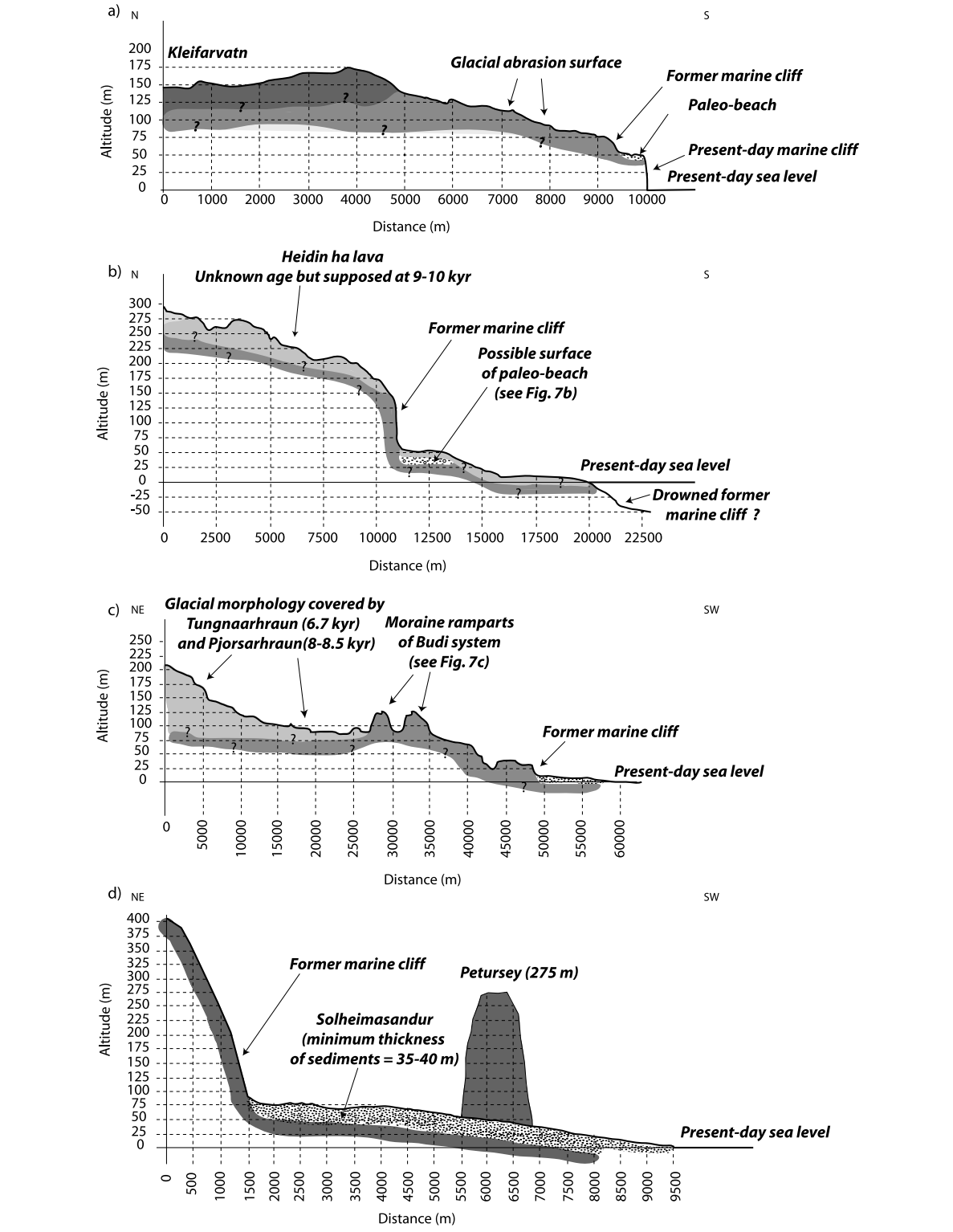
a)
N
S
Kleifarvatn
Glacial abrasion surface
Former marine cliff
Paleo-beach
Present-day marine cliff
Present-day sea level
Altitude (m)
Distance (m)
b)
N
S
Heidin ha lava
Unknown age but supposed at 9-10 kyr
Former marine cliff
Possible surface
of paleo-beach
(see Fig. 7b)
Present-day sea level
Drowned former
marine cliff ?
Altitude (m)
Distance (m)
c)
NE
SW
Glacial morphology covered by
Tungnaarhraun (6.7 kyr)
and Pjorsarhraun(8-8.5 kyr)
Moraine ramparts
of Budi system
(see Fig. 7c)
Former marine cliff
Present-day sea level
Altitude (m)
Distance (m)
d)
NE
SW
Former marine cliff
Petursey (275 m)
Solheimasandur
(minimum thickness
of sediments = 35-40 m)
Present-day sea level
Altitude (m)
Distance (m)
Holocene sediments
Abandoned beach surface
Basic and intermediate lavas, postglacial, historic, younger than 1,100 years
Basic and intermediate lavas, postglacial, prehistoric, older than 1,100 years
Basic and intermediate interglacial and supraglacial lavas with intercalated sediments, Upper Pleistocene, younger than 0.8 Ma
Basic and intermediate hyaloclastite, pillow-lava and associated sediments, Upper Pleistocene, younger than 0.8 Ma

**Figure 8**

gation at the base of the present-day cliff shows that the basement is at least 35 to 40 m below the topographic surface.

### 4.3. Glacial and Marine Level Map

[30] Observations were gathered on a map with additional data to obtain a complete scheme of the Holocene evolution of the southwestern part of Iceland (Figure 9a). Numerous glacial striations, samples of dated marine organisms and ages of postglacial lava flows along the southwestern coast were plotted as well. Numerous marine organisms were found from Hveragerdi to Hella and from the present-day shoreline to the moraine system of Budi [*Hjartarson and Ingolfsson*, 1988]. The marine fossils show that the sea invaded the land as far as 40 km from the present-day shoreline, at an elevation of +70–80 m. The ages of postglacial lava flows provided good constrains for time evolution of the observed surfaces in the Reykjanes peninsula and around Selfoss. They formed in subaerial conditions, which allow the sea level and glacial extent at the time of their formation to be constrained. The numerous glacial striations constrain the extent of the glaciers, but it is impossible to date these features.

[31] All these observations allowed us to map three levels: two ancient shorelines and the glacial extent of the ice cap on bedrock (Figure 9b). These markers do not permit to map the sea ice. Three domains with different characteristics are clearly distinguishable: the Reykjanes peninsula, the central part of the study area and the Vik area.

[32] In the Reykjanes peninsula there are two marine notches: one cropping out at an elevation of +50 m, forming clear marine cliffs with a tidal flat at the base, and a submarine one at a depth of −40 m, inferred from drowned postglacial lava flows, knickpoints of the seafloor and breaking waves offshore. The maximal extent of the ice cap is at an elevation of +90 m according to the position of glacial striations and to the nature of hyaloclastite mountains.

[33] The central domain, ranging from Hveragerdi to Hvolsvöllur, has unclear morphological boundaries because of successive jokülhlaups along the Thjorsa and Ytri-Ranga rivers. Nevertheless, the age of these surfaces is constrained by marine fossils and dated moraines. A high marine level is at an elevation of +70–80 m, locally +100 m (maximal altitude of marine shells), even +110 m in form of a marine notch incised in the outer terminal moraine of the Budi system as the trace of the upper marine limit. The maximal extent of the late Glacial ice cap seems stabilized at +90 to 105 m, well constrained by the outer terminal moraine of Budi. A low marine notch at −40 m is not well expressed on the bathymetry, but is well constrained off Eyrarbakki by the postglacial lava flow Thjorsarhraun emplaced in aerial conditions at 8.5 ka BP. Our observations also showed a marine notch at +15 m.

[34] The eastern domain is south of Eyjafjallajökull toward Vik. It consists of a high marine cliff, whose base has variable elevation (from +15 m to 75 m), and wide fluvioglacial deposit with unknown thickness. Glacial striations mark the extent of ice cap on the bedrock at the top of the cliffs, at an elevation higher than +400 m. A scarp at −40 m probably goes around the Vestmann Islands according to the rough bathymetric data. Our high marine notches are similar to those determined by *Ingolfsson* [1991], given by *Geirsdottir et al.* [2000].

[35] Radiocarbon ages on marine shells and ages of postglacial lava flows [*Thordarson and Hoskuldsson*, 2002] give the ages of the marine and glacial levels (Figure 9b). The age of the high marine level seems to be 10,000 years BP, which is coherent with the values published by *Ingolfsson et al.* [1995]. Indeed, marine shells of the central domain were dated between 9000 and 10,000 years BP [*Hjartarson and Ingolfsson*, 1988]. They cover a wide zone from Hveragerdi and Hvolsvöllur, which was submerged by the sea during this period. Postglacial lava flows of the Reykjanes peninsula were dated at about 9000–10,000 years BP [*Thordarson and Hoskuldsson*, 2002]. The emplacement of these lava flows in aerial conditions is coherent with an earlier high sea level close to 10,000 years BP. We assume an age of 10,000 years BP for the glacial boundary in the central part, which is consistent with the age of the moraine system of Budi [*Geirsdottir et al.*, 1997]. The accurate age of the ice extent is less constrained in the western and eastern segments because of sea ice and bad deglaciation timing. We assumed an age of 8500 years BP for the low marine level constrained by the age of the postglacial lava flow Thjorsarhraun, emplaced in aerial conditions near Eyrarbakki.

[36] Sea level rose step by step with accelerations during the late glacial event [*Peltier and Fairbanks*, 2006]. A new glacial loading occurred mostly sensitive in the middle zone during the Younger Dryas readvance. The upper marine limit yields 10,000 years BP since marine shells could live in the area of Hveragerdi and Hella, probably during the cooling of the Younger Dryas (outer Budi Advance) limiting the turbidity of glacial outlets. When the deglaciation began, the isostatic rebound imposed a fast retreat of the shoreline to the low marine notch circa 8500 years BP. This low sea level built a tidal notch along the southern coast of Reykjanes peninsula. Postglacial lava flowed in this area and near Selfoss (Thjorsarhraun lava) in sea- and ice-free conditions. After 8500 years BP, the sea level continued to rise. The drowned lava records this Holocene flooding in Thorlakshöfn and Hafnir.

### 4.4. Vertical Motions

[37] Amount and rates of vertical motions allow distinguishing the three domains of the southwestern coast of Iceland by means of location and elevation of the different marine levels (Figure 9b) and of the method presented in section 4.2. The results are presented in Table 1 and summarized in Figure 10.

[38] An important uplift affected Iceland from 10,000 to 8500 years BP as a direct answer of the fast retreat of the Late Glacial ice cap. Vertical motions and rates varied from west to east. The uplift reached 113.5 m with a rate of 6.8–7.6 cm/a in the Reykjanes peninsula, 157.5 m with a rate of 8.2–10.5 cm/a in the central domain, and ranged from 67 to 132.5 m with a rate of 4.5 to 8.8 cm/a in the eastern domain. For this latter part located around Vik, estimations were

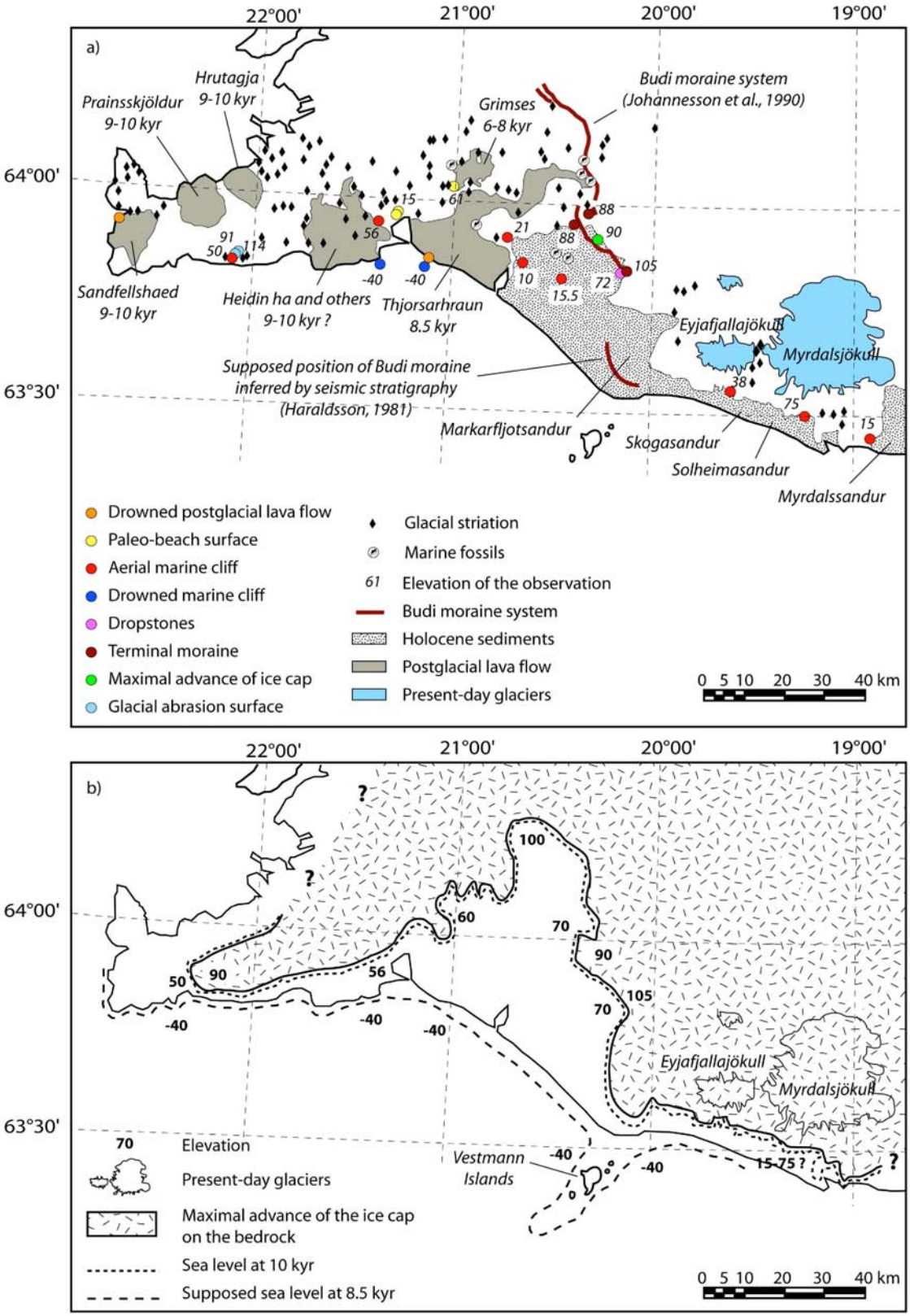


**Figure 9.** (a) Synthetic map of observations done on the field and additional data. (b) Map of maximal glacial advance on the bedrock and sea levels at 10 ka and 8.5 ka BP. The numbers indicate the elevation of the main markers.

**Table 1.** Vertical Motion Amounts and Rates Along the Southwestern Coast of Iceland[a]

| | CR/S | Δz/r | Reykjanes Peninsula | Hveragerdi-Hvolsvöllur | Vik | Absolute Marine Sea Level |
|---|---|---|---|---|---|---|
| 10–8.5 ka | CR | Δz | 102.5–108.5 m | 122.5–152.5 m | 67.5–127.5 | 12.5 ± 5 m |
| | | r | 6.8–7.2 cm/a | 8.2–10.2 cm/a | 4.5–8.5 cm/a | 0.8 ± 0.3 cm/a |
| | S | Δz | 107.5–113.5 m | 127.5–157.5 m | 72.5–132.5 m | 17.5 m |
| | | r | 7.2–7.6 cm/a | 8.5–10.5 cm/a | 4.8–8.8 cm/a | 1.26 cm/a |
| 8.5 ka-actual | CR | Δz | −17.5 ± 5 m | −17.5 ± 5 m | −17.5 ± 5 m | 22.5 ± 5 m |
| | | r | −0.2 ± 0.05 cm/a | −0.2 ± 0.05 cm/a | −0.2 ± 0.05 cm/a | 0.3 ± 0.05 cm/a |
| | S | Δz | −2.5 ± 5 m | −2.5 ± 5 m | −2.5 ± 5 m | 37.5 m |
| | | r | −0.03 ± 0.05 cm/a | −0.03 ± 0.05 cm/a | −0.03 ± 0.05 cm/a | 0.4 cm/a |

[a]Time periods correspond to those chosen for the marine stages. Eustatic curves used are: CR, Coral Reef; S, SPECMAP. $\Delta z > 0$ means uplift (m), $\Delta z < 0$ means subsidence (m), and r is motion rate (cm/a).

calculated using the elevations measured at the bottom of marine cliffs. We were not able to subtract the thickness of Holocene sediments because this data remains unknown. According to our additional electric data, we can assume that the thickness of the sandurs is more than 40 to 45 m and so the bottom of the cliff is around +15–30 m, which means that uplift rates are about 4.5–6 cm/a.

[39] During this period 10,000–8500 years BP, the uplift rate in southern Iceland was faster than the sea level rise in a well glaciated zone during the Younger Dryas forcing a fast drop of the relative sea level. The end of this fast rebound occurred approximately at 8500 years BP allowing the shaping of a new marine cliff. This stage could correspond to a period where the uplift and the sea level had similar rates, generating an apparent steady state in this region. Since 8500 years BP, the estimation indicates a slight downward motion from 2.5 to 17.5 m (Table 1). The sea level keeps rising, submerging the emerged coastal plain and the postglacial lava flows as observed in Thorlakshöfn and Hafnir (Reykjanes peninsula). Therefore, Iceland subsided with rates of a few mm/a. These new data sets allow us to distinguish subsidence and drowning due to a rise of sea level, considering the absolute sea level evolution. Thus, the positive or negative value of the motion is in an absolute reference.

## 5. Discussion

[40] This field analysis allowed us to quantify the effect of ice unloading versus sea level rise during the Holocene in the southwestern coast of Iceland. This area has undergone important uplift since 10,000 years BP. The uplift ranged from 67.5 m to 157.5 m depending on the area, from 10 to 8.5 ka BP, which corresponds to an uplift rate of 4.5 to 10.5 cm/a. Thus the evolution is characterized by two stages indicating different behaviors: a first fast rebound phase and a roughly steady state phase.

[41] The rifting contribution to the vertical motion is difficult to estimate. However, the results show that vertical motions seem independent of the regional geodynamic context. The Reykjanes domain was the most affected by the rifting processes, while the Vik domain was the less affected since located outside of the active zone. *Hofton and Foulger* [1996a, 1996b] estimated an uplift rate of 2 cm/a in the northern rift for recent periods. This value is largely lower than those obtained during the first stage (8–10 cm/a) and largely higher than those of the second quiet stage (around 1 mm/a). Furthermore, the uplift rate during the last stage is similar in the three domains, whatever the geodynamic pattern. Thus, the extensional deformation contributes slightly to the vertical motion at the regional scale. The influence is prominent close to the normal faults at local scale, i.e., at 10-m scale and not at 100-km scale. This result is more compatible with a model of unsteady rollovers [*Bourgeois et al.*, 2005] than with large and tilted blocks. Thus, the postglacial rebound mainly appears to contribute to the vertical motion. The amount of upward displacement is directly proportional to the ice load. One kilometer of ice generates approximately a 300 m subsidence, which implies that the glacio-isostatic rebound cannot excess 300 m in this case. This simple estimate assumes a local compensation and a steady state system before the ice loading. Therefore, the rebound amount gives an inverted imprint of the ice loading at a local scale. In this study case, it means that the ice thickness may reach at least 100 m on the coastal plain.

[42] The data allow distinguishing two periods of vertical displacements. The first stage, which occurred between 10,000 and 8500 years BP, corresponds to a fast uplift with rates between 5 and 10 cm/a, consecutive to the postglacial rebound. A similar study was done in the area of Reykjavik [*Ingolfsson et al.*, 1995], using the same method of eustatic changes associated to shoreline displacements: it provided similar results with an uplift rate of 6.9 cm/a for the period 10,300–9400 years BP. The uplift rates we determined in this study are about twice higher than those determined for other glacial areas: 3.3 cm/a at Jameson Land, east Greenland [*Björk et al.*, 1994], 3.3 cm/a in the north of Spitsbergen archipelago [*Boulton*, 1979], 4.5 cm/a south of Norway [*Anundsen*, 1985]. These values were calculated with similar methods for periods at the onset of deglaciation. *Kjemperud* [1986] has studied shoreline displacements in central Norway. There was a huge uplift between 10,000 and 8500 years BP with uplift rates reaching 4.5–5.8 cm/a.

[43] The second stage determined in Iceland corresponds to a slow subsidence with motion rates 1 to 2 orders lower

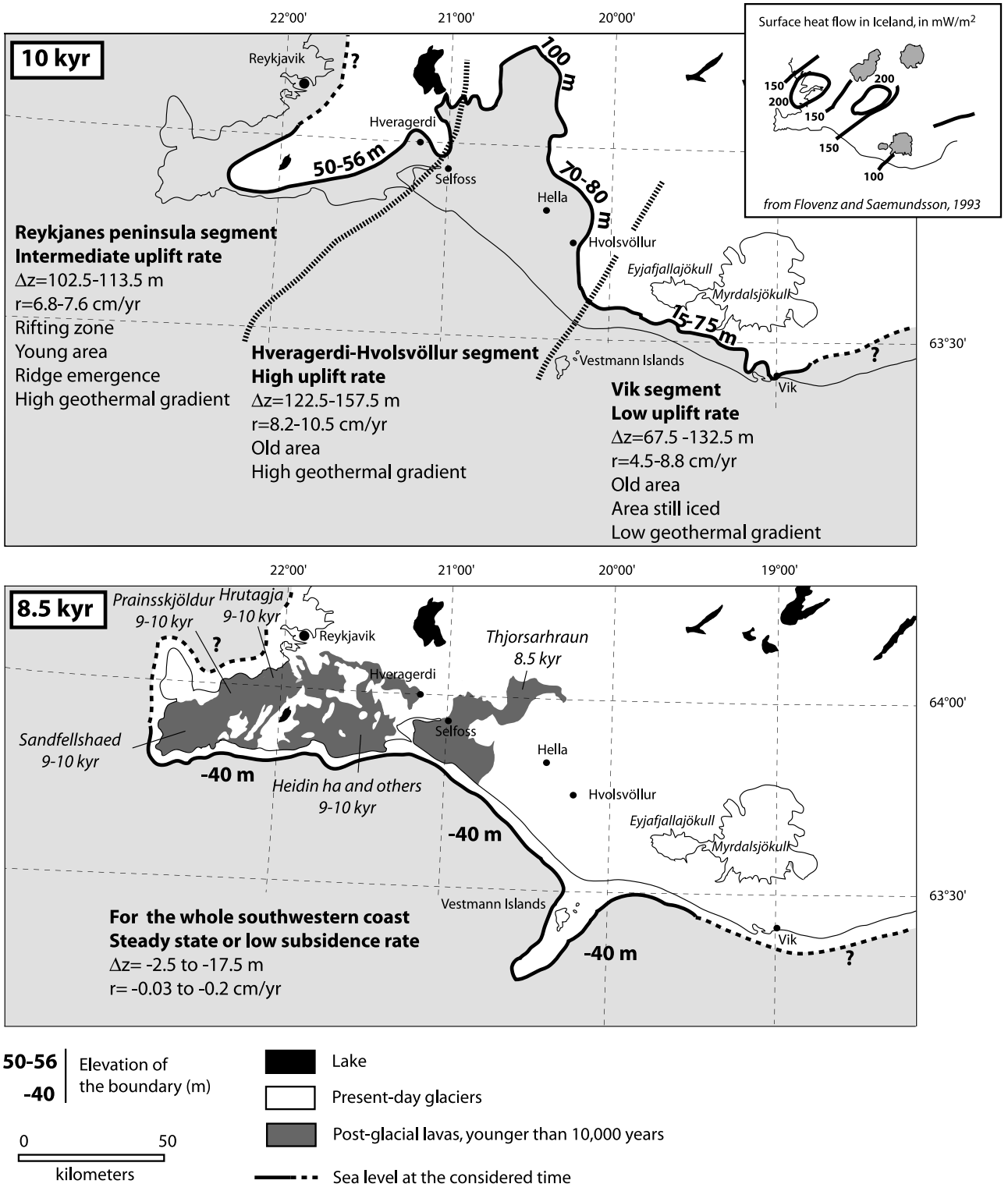


**Figure 10.** Synthetic maps showing the sea levels at 10 ka and at 8.5 ka BP. Δz, uplift (positive values) or subsidence (negative values) amount; r, motion rate.

(few mm/a) since 8500 years BP. The estimation provided some negative values that mean a true downward motion of Iceland and not an uplift slower than the sea rise. The uplift is close to zero within the given accuracy as compared to the SPECMAP curve. Thus, in this case, Iceland is at steady state since 8500 years BP. The Coral Reef curve predicts a subsidence since 8500 years BP that means an evolution completely independent of the glacial rebound. The origin

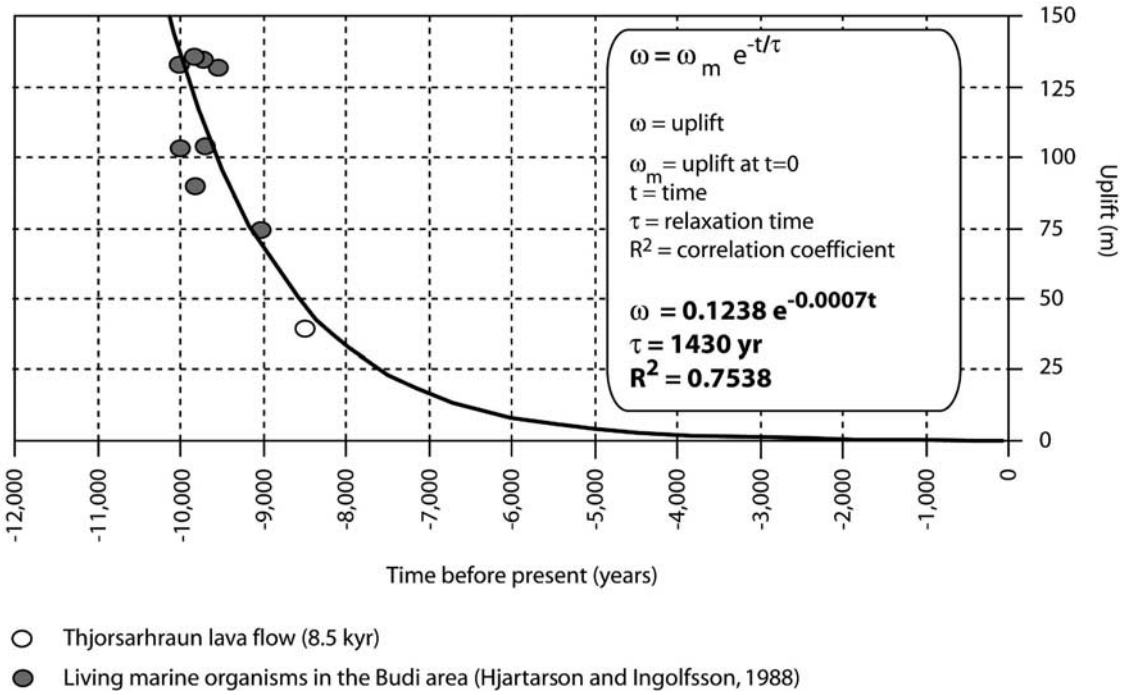


**Figure 11.** Uplift of living marine organisms found in the Budi area and of the Thjorsarhraun lava flow versus time and estimation of the relaxation time of the postglacial rebound.

of this downward motion is unknown. However, a magmatic-volcanic loading by surface flooding and/or by underplating can be advanced. A complete analysis done around Iceland could probably constrain the true scale of this process. These high postglacial uplift rates are compatible with fast glacial retreat. Indeed, the location of Iceland in North Atlantic favors a fast retreat of the ice sheet related to the recovery of the thermohaline circulation [*Van Vliet-Lanoë et al.*, 2007]. The consequence is that the effects of an ice load in an oceanic context are more important than in a continental domain [*Ingolfsson et al.*, 1995].

[44] The results reveal a rebound segmentation into three blocks along the southwestern coast of Iceland, with different characteristics (Figure 10). The central part from Hveragerdi to Hvolsvöllur has undergone the highest uplift rates (locally reaching 10 cm/a) and vertical displacements (150 m). This area is affected by the highest uplift amount, which means that it was loaded by a thick ice sheet as compared to other studied areas. At the Younger Dryas, the sea invaded the coastal plains because of the ice load occurring in Iceland. The western and the eastern segments have undergone a lower uplift indicating a thinner or an unsteady ice sheet. The Reykjanes peninsula is a young active rift zone with four eruptive swarms, which produced numerous postglacial lava flows. This area was probably not completely covered by the ice cap during the Younger Dryas [*Ingolfsson et al.*, 1997], and vertical motions created by rifting could have balanced postglacial rebound. This generates unsteady ice sheet that may melt with its own dynamics. Finally, the Vik area is presently partly iced with Eyjafjallajökull (80 $km^2$) and Myrdalsjökull (600 $km^2$) glaciers. Coastal surfaces are important fluvio-glacial drift plains with numerous sandurs (Skogasandur, Solheimasandur and Myrdalssandur). The calculated uplift rates suggest that smaller motions (4.5 to 6 cm/a) probably occurred because of a persistent ice load during the Younger Dryas. The uplift amount that provides an indirect image of the ice load is compatible with the thin ice cover proposed by *Ingolfsson et al.* [1997] in Reykjanes peninsula and with the closeness of the shoreline. The uplift motion segmentation fits with an uplift rate segmentation, the median segment being characterized by a higher rate than the two others with differences up to 50%.

[45] The uplift rate is directly controlled by the timing of the glacial retreat or by the viscosity of the asthenospheric layers. The first hypothesis can be reasonably rejected because the deglaciation should follow the same timing in the whole southwestern area that displays a homogeneous configuration (closeness to the shoreline, main rough orientation, similar ocean boundary conditions…). Thus, we investigated the hypothesis of a viscosity variation of deep layers. The regional geothermal gradient could provide a good proxy of the viscosity variations. This area also displays an important geothermal activity since the surface heat flow varies from 150 mW $m^{-2}$ near the present-day shoreline to 200 mW $m^{-2}$ south of Langjökull [*Flovenz and Sæmundsson*, 1993]. *Bourgeois* [2000] showed a correlation between the location of geothermal anomalies and the main ice routes. On the southwestern coast, the geothermal heat flux ranges from 100 mW/$m^2$ to more than 200 mW/$m^2$. The highest heat fluxes (>150 mW/$m^2$) are located from Selfoss to Hvolsvöllur that corresponds to the central segment. On both

sides, they reach lower values. Therefore, a correlation appears between rebound segmentation and distribution of the surface heat flux.

[46] The relaxation time of the glacial rebound can be estimated and by consequence the asthenosphere viscosity through timing and uplift calculations in the central zone. We obtained a relaxation time of 1430 years from the data (Figure 11), which is consistent with our hypothesis of a fast postglacial rebound between 10,000 and 8500 years BP. This relaxation time is twice less than classical relaxation time [*Dyke and Peltier*, 2000; *Japsen*, 2000; *Fjeldskaar et al.*, 2000; *Watts*, 2001; *Turcotte and Schubert*, 2002]. However, it has to be linked with the deformation wavelength. The relaxation time for Fennoscandia was around 3500 years, and affected a region wider than 1000 km. In Iceland, this uplift has a wavelength of around 500 km for a relaxation time of 1430 years. The ratio wavelength versus relaxation time is quite the same for Fennoscandia and Iceland. Thus there is no visible effect of the Icelandic hot spot in terms of relaxation time.

[47] From the relaxation time $\tau$ we estimated the asthenosphere viscosity $\mu$, based on two models: (1) $\tau = \frac{4\pi\mu}{\rho g \lambda}$ from *Turcotte and Schubert* [2002], in the case of a viscous half-space model with a full isostatic compensation; and (2) $\tau = \frac{\mu}{\rho g n R_T}(2n^2 + 4n + 3)$ from *Peltier* [1974] and *Cathles* [1975], which solves the problem for a viscous and homogeneous sphere, with $\rho$ the asthenosphere density, $g$ the gravitational acceleration (9.81 m $s^{-2}$), $\lambda$ the deformation wavelength (500 km for Iceland), $n$ the Legendre degree equal to 16 for a load of 500-km wavelength and $R_T$ the Earth's radius (6371 km).

[48] The boundary between the lithosphere and the asthenosphere is defined by the depth of the 1200°C isotherm that corresponds to a abrupt decrease of the viscosity at depth. This isotherm is located 30–40 km under the Reykjanes peninsula and 60–70 km under the Vik area. The depth of the Moho is 10–15 km in the west and 25–30 km in the east [*Darbyshire et al.*, 2000; *Kaban et al.*, 2002]. These observations indicate that the boundary between the lithosphere and the asthenosphere is mainly located in the upper parts of the mantle, which have densities $\rho$ of 3050–3280 kg $m^{-3}$ [*Darbyshire et al.*, 2000; *Kaban et al.*, 2002]. Thus, we obtain viscosities of (1) 5.4–5.8 $\times$ $10^{19}$ Pa s, and (2) 2.4–2.6 $\times$ $10^{20}$ Pa s, respectively. These viscosity values are similar or a little bit higher than the values calculated on 10-year timescales with other methods in Iceland: $10^{19}$ Pa s [*Sigmundsson*, 1991], $10^{18}$ Pa s with gravimetrical measurements between 1991 and 2000 [*Jacoby et al.*, 2001], 7 $\times$ $10^{16}$–3 $\times$ $10^{18}$ Pa s with measurements at Langisjor lake between 1959 and 1991 [*Thoma and Wolf*, 2001], $10^{17}$ Pa s with GPS measurements [*Sjöberg et al.*, 2004], 3–8 $\times$ $10^{18}$ Pa s with GPS measurements around the Vatnajökull ice cap [*Pagli et al.*, 2006], 0.3–30 $\times$ $10^{18}$ Pa s using post-rifting motions after the Krafla event [*Einarsson et al.*, 2006]. For the Fennoscandia, *Fjeldskaar* [1994, 1997, 2000] obtained viscosities of 1.0–2.0 $\times$ $10^{21}$ Pa s for the lower mantle, 0.7–1.0 $\times$ $10^{21}$ Pa s for the upper mantle and of 1.3 $\times$ $10^{19}$ Pa s for the asthenosphere. For the south of Alaska, *Larsen et al.* [2004] determined a viscosity of 4 $\times$ $10^{20}$ Pa s for the upper mantle and of 1.4 $\times$ $10^{19}$ Pa s for the asthenosphere. The upper mantle viscosity estimated in this study is lower than that determined for upper mantle (1–3 $\times$ $10^{20}$ Pa s) in Hawaiian hot spot [*Zhong and Watts*, 2002].

[49] Thus, this study reveals no difference in terms of viscosity between the asthenosphere located in a hot spot context such as Iceland and the one of a continent as Fennoscandia. However, the main difference is the depth of the boundary (isotherm 1200°C) between the lithosphere and the asthenosphere: 30 to 60 km beneath Iceland [*Darbyshire et al.*, 2000; *Kaban et al.*, 2002] versus 110–150 km beneath the Fennoscandian shield [*Martinec and Wolf*, 2005]. The thin lithosphere of Iceland is responsible of the short wavelength of the flexural behavior. The hot spot effect is more visible on lithosphere thicknesses than on asthenosphere viscosities. One direct mechanical consequence of this thin lithosphere is that the lithosphere is third or fourth weaker than in continental domains.

## 6. Conclusions

[50] The southwestern coast of Iceland is a perfect area for studying the relationships between geodynamic context and glacial rebound. We have studied vertical motions of the southwestern coastal plains of Iceland during the Holocene, using markers of sea level and eustatic variation. We pointed out two periods of vertical displacements: a first one with high-amplitude motions (8–10 cm/a) between 10,000 and 8500 years BP just after the deglaciation, and a second stage of steady state or subsidence (a few mm/a) from 8500 years BP to present. We observe a fast and partitioned rebound of the southwestern coast with variable uplift rates: (1) a central zone with highly seismic activity and which was subject to a high surface heat flow and the most important uplift rates (8–10 cm/a), (2) the young Reykjanes peninsula (7 cm/a), which was probably less glaciated and subject to important rifting processes, and (3) the old basement area of Vik, which was still iced at the Younger Dryas, with low uplift rates (4–6 cm/a). This uplift distribution is interpreted as resulting from the combination of the ice loading and of, above all, the rheological behavior of the crust that is weakest and hottest in the central segment than outside. This rate of isostatic rebound allowed viscosity estimations for the asthenosphere between 5.4 and 5.8 $\times$ $10^{19}$ and 2.4–2.6 $\times$ $10^{20}$ Pa s depending on numerical method. These values are slightly higher to those determined for Iceland with other methods at ten-year timescales and are quite similar to those determined for Fennoscandia, where there is a thicker lithosphere (110–150 km, depth of the 1200°C isotherm) and a wavelength twice higher (1000 km). Therefore, this study reveals that the uppermost asthenosphere has roughly the same viscosity in Iceland than in other parts of the world. However, its depth is shallower, which implies a shorter wavelength for the flexural response. At shorter scale, the geodynamic pattern in terms of geothermal gradient emphasizes the rebound response.

[51] **Acknowledgments.** The authors thank IPEV Institute for its constant financial support (program 316) and INSU program "Relief de la Terre" for a field trip grant. We greatly appreciate helpful discussions with F. Bergerat (UPMC–Paris), F. Guillocheau (Géosciences Rennes), J. Braun (Géosciences Rennes), and A. Dia (Géosciences Rennes). We thank P. R. Cobbold (Géosciences Rennes) for constructive reading of this paper.

## References

Andrews, J. T., and G. Helgadottir (2003), Late Quaternary ice cap extent and deglaciation, Hunafloafall, northwest Iceland: Evidence from marine cores, *Arct. Antarct. Alp. Res.*, *35*, 218–232, doi:10.1657/1523-0430(2003)035[0218:LQICEA]2.0.CO;2.

Andrews, J. T., et al. (2000), The N and W Iceland shelf: Insights into the Last Glacial Maximum ice extent and deglaciation based on acoustic stratigraphy and basal radiocarbon AMS dates, *Quat. Sci. Rev.*, *19*, 619–631, doi:10.1016/S0277-3791(99)00036-0.

Anundsen, K. (1985), Changes in shore-level and ice-front position in Late Weichsel and Holocene, southern Norway, *Nor. Geogr. Tidsskr.*, *39*, 205–225.

Bellou, M., F. Bergerat, J. Angelier, and C. Homberg (2005), Geometry and segmentation mechanisms of the surface traces associated with the 1912 Selsund earthquake, Southern Iceland, *Tectonophysics*, *404*, 133–149, doi:10.1016/j.tecto.2005.04.005.

Björk, S., O. Bennike, O. Ingolfsson, L. Barnekow, and D. Penney (1994), Lake Boksehandsken's earliest postglacial sediments and their palaeoenvironmental implications, Jameson Land, East Greenland, *Boreas*, *23*, 459–472.

Boulton, G. (1979), Glacial history of the Spitsbergen archipelago and the problems of a Barents Shelf ice sheet, *Boreas*, *8*, 31–57.

Bourgeois, O. (2000), Processus d'extension lithosphérique en Islande, interactions avec les calottes glaciaires quaternaires, Ph.D. thesis, 238 pp., Univ. de Rennes, Rennes, France.

Bourgeois, O., O. Dauteuil, and E. Hallot (2005), Rifting above a mantle plume: The Icelandic Plateau, *Geodin. Acta*, *18*(1), 59–80, doi:10.3166/ga.18.59-80.

Braun, J., and C. Beaumont (1989), Dynamical models of the role of crustal shear zones in asymmetric continental extension, *Earth Planet. Sci. Lett.*, *93*, 405–423, doi:10.1016/0012-821X(89)90039-3.

Cathles, L. M. (1975), *The Viscosity of the Earth's Mantle*, 386 pp., Princeton Univ. Press, Princeton, N. J.

Chéry, J., F. Lucazeau, M. Daignières, and J.-P. Vilotte (1992), Large uplift of rift flanks: a genetic link with lithospheric rigidity?, *Earth Planet. Sci. Lett.*, *112*, 195–211, doi:10.1016/0012-821X(92)90016-O.

Clifton, A., F. Sigmundsson, K. L. Feigl, G. Gudmundsson, and T. Arnadottir (2002), Surface effects of faulting and deformation resulting from magma accumulation at the Hengill triple junction, SW Iceland, 1994–1998, *J. Volcanol. Geotherm. Res.*, *115*, 233–255, doi:10.1016/S0377-0273(01)00319-5.

Darbyshire, F., R. S. White, and K. F. Priestley (2000), Structure of the crust and upper mantle of Iceland from a combined seismic and gravity study, *Earth Planet. Sci. Lett.*, *181*, 409–428, doi:10.1016/S0012-821X(00)00206-5.

Dauteuil, O., J. Angelier, F. Bergerat, S. Verrier, and T. Villemin (2001), Deformation partitioning inside a fissure swarm of the northern Icelandic rift, *J. Struct. Geol.*, *23*(9), 1359–1372, doi:10.1016/S0191-8141(01)00002-5.

Dauteuil, O., J. Bouffette, F. Tournat, B. Van Vliet-Lanoë, J.-C. Embry, and Y. Quété (2005), Holocene deformation outside the active zone of north Iceland, *Tectonophysics*, *404*, 203–216, doi:10.1016/j.tecto.2005.04.009.

DeMets, C., R. G. Gordon, D. F. Argus, and S. Stein (1994), Effects of recent revisions to the geomagnetic time scale on estimates of current plate motions, *Geophys. Res. Lett.*, *21*(20), 2191–2194, doi:10.1029/94GL02118.

Dyke, A. S., and W. R. Peltier (2000), Forms, response times and variability of relative sea-level curves, glaciated North America, *Geomorphology*, *32*, 315–333, doi:10.1016/S0169-555X(99)00102-6.

Einarsson, T., and K. Albertsson (1988), The glacial history of Iceland during the past three million years, *Philos. Trans. R. Soc. Ser. B*, *318*, 637–644, doi:10.1098/rstb.1988.0027.

Einarsson, P., F. Sigmundsson, E. Sturkell, T. Arnardóttir, R. Pedersen, C. Pagli, and H. Geirsson (2006), Geodynamics signals detected by geodetic methods in Iceland, in *Geburtstages und der Verabschiedung in den Ruhestand*, *Wiss. Arb. Fachrichtung Geod. Geoinf. Univ. Hannover*, *258*, 39–57.

Fjeldskaar, W. (1994), Viscosity and thickness of the asthenosphere detected from the Fennoscandian uplift, *Earth Planet. Sci. Lett.*, *126*, 399–410, doi:10.1016/0012-821X(94)90120-1.

Fjeldskaar, W. (1997), Flexural rigidity of Fennoscandia inferred from the postglacial uplift, *Tectonics*, *16*(4), 596–608, doi:10.1029/97TC00813.

Fjeldskaar, W. (2000), How important are elastic deflections in the Fennoscandian postglacial uplift?, *Nor. Geol. Tidsskr.*, *80*, 57–62, doi:10.1080/00291600750042681.

Fjeldskaar, W., C. Lindholm, J. Dehls, and I. Fjeldskaar (2000), Postglacial uplift, neotectonics and seismicity in Fennoscandia, *Quat. Sci. Rev.*, *19*, 1413–1422, doi:10.1016/S0277-3791(00)00070-6.

Flovenz, O. G., and K. Sæmundsson (1993), Heat flow and geothermal processes in Iceland, *Tectonophysics*, *225*, 123–138, doi:10.1016/0040-1951(93)90253-G.

Foulger, G. R., Z. Du, and B. R. Julian (2003), Icelandic-type crust, *Geophys. J. Int.*, *155*, 567–590, doi:10.1046/j.1365-246X.2003.02056.x.

Garcia, S., N. O. Arnaud, J. Angelier, F. Bergerat, and C. Homberg (2003), Rift jump process in northern Iceland since 10 Ma from $^{40}Ar/^{39}Ar$ geochronology, *Earth Planet. Sci. Lett.*, *214*, 529–544, doi:10.1016/S0012-821X(03)00400-X.

Geirsdottir, A., J. Hardardóttir, and J. Eiriksson (1997), The depositional history of the Younger Dryas-Preboreal Búdi moraines in South-Central Iceland, *Arct. Alp. Res.*, *29*(1), 13–23, doi:10.2307/1551832.

Geirsdottir, A., J. Hardardóttir, and A. E. Sveinbjörnsdóttir (2000), Glacial extent and catastrophic meltwater events during the deglaciation of Southern Iceland, *Quat. Sci. Rev.*, *19*, 1749–1761, doi:10.1016/S0277-3791(00)00092-5.

Gudmundsson, A., L. B. Marinoni, and J. Marti (1999), Injection and arrest of dykes: Implications for volcanic hazards, *J. Volcanol. Geotherm. Res.*, *88*, 1–13, doi:10.1016/S0377-0273(98)00107-3.

Gudmundsson, M. T., A. Bonnel, and K. Gunnarsson (2002), Seismic soundings of sediment thickness on Skeidarársandur, SE Iceland, *Jokull*, *51*, 53–64.

Guilcher, A., J.-C. Bodéré, A. Coudé, J. D. Hansom, A. Moign, and J.-P. Peulvast (1994), The strandflat problem in five high latitude countries, in *Cold Climate Landforms*, edited by D. J. A. Evans, pp. 47–69, John Wiley, Hoboken, N. J.

Haraldsson, H. (1981), The Markarfljot sandur area, southern Iceland: Sedimentological, petrographical and stratigraphical studies, *Striae*, *15*, 1–58.

Helgason, J. (1984), Frequent shifts of the volcanic zone in Iceland, *Geology*, *12*, 212–216, doi:10.1130/0091-7613(1984)12<212:FSOTVZ>2.0.CO;2.

Helgason, J. (1985), Shifts of the plate boundary in Iceland: Some aspects of Tertiary volcanism, *J. Geophys. Res.*, *90*(B12), 10,084–10,092.

Henriot, O., T. Villemin, and F. Jouanne (2001), Long period interferograms reveal 1992–1998 steady rate of deformation at Krafla volcano (north Iceland), *Geophys. Res. Lett.*, *28*(6), 1067–1070, doi:10.1029/2000GL011712.

Hjartarson, A., and O. Ingolfsson (1988), Preboreal glaciation of Southern Iceland, *Jokull*, *38*, 1–13.

Hofton, M. A., and G. R. Foulger (1996a), Postrifting anelastic deformation around the spreading plate boundary, north Iceland: 1. Modeling the 1987–1992 deformation field using a viscoelastic Earth structure, *J. Geophys. Res.*, *101*(B11), 25,403–25,421, doi:10.1029/96JB02466.

Hofton, M. A., and G. R. Foulger (1996b), Postrifting anelastic deformation around the spreading plate boundary, north Iceland: 2. Implications of the model derived from the 1987–1992 deformation field, *J. Geophys. Res.*, *101*(B11), 25,423–25,436, doi:10.1029/96JB02465.

Hoppe, G. (1982), The extent of the last inland ice sheet of Iceland, *Jokull*, *32*, 3–11.

Hopper, J. R., and R. W. Buck (1998), Styles of extensional decoupling, *Geology*, *26*, 699–702, doi:10.1130/0091-7613(1998)026<0699:SOED>2.3.CO;2.

Ingolfsson, O. (1991), A review of the late Weichselian and early Holocene glacial and environmental history of Iceland, in *Environmental Change in Iceland: Past and Present*, edited by J. L. Maizels and C. J. Caseldine, pp. 13–29, Kluwer Acad., Dordrecht, Netherlands.

Ingolfsson, O., and H. Norddahl (1994), A review of the environmental history of Iceland 13,000–9,000 yr BP, *J. Quat. Sci.*, *9*(2), 147–150, doi:10.1002/jqs.3390090208.

Ingolfsson, O., and H. Norddahl (2001), High relative sea level during the Bolling Interstadial in western Iceland: A reflection of ice-sheet collapse and extremely rapid glacial unloading, *Arct. Antarct. Alp. Res.*, *33*, 231–243, doi:10.2307/1552224.

Ingolfsson, O., H. Norddahl, and H. Haflidason (1995), Rapid isostatic rebound in southwestern Iceland at the end of the last glaciation, *Boreas*, *24*, 245–259.

Ingolfsson, O., S. Björk, H. Haflidason, and M. Rundgren (1997), Glacial and climatic events in Iceland reflecting regional North Atlantic climatic shifts during the Pleistocene-Holocene transition, *Quat. Sci. Rev.*, *16*, 1135–1144, doi:10.1016/S0277-3791(97)00007-3.

Jacoby, W. R., S. Bürger, P. Smilde, and H. Wallner (2001), Temporal gravity variations observed in SE Iceland, *InterRidge News*, *10*(1), 52–55.

Japsen, P. (2000), Investigation of multi-phase erosion using reconstructed shale trends based on sonic data, Sole Pit axis, North Sea, *Global Planet. Change*, *24*(3–4), 189–210, doi:10.1016/S0921-8181(00)00008-4.

Johannesson, H., and K. Saemundsson (1998), Geological map of Iceland: Bedrock geology, 1/500,000, map, Icelandic Mus. of Nat. Hist., Reykjavik.

Johannesson, H., S. P. Jakobsson, and K. Saemundsson (1990), Geological map of Iceland, sheet 6, South Iceland, 3rd ed., map, Icelandic Mus. of Nat. Hist., Reykjavik.

Jouet, G. (2003), Origines des sequences sédimentaires emboîtées sur la marge externe du Golfe du Lion du stade isotopique 3 à l'actuel (derniers 50000 ans), Mem. de DEA, Univ. de Bretagne Occident., Brest, France.

Jouet, G., S. Berné, M. Rabineau, M. A. Bassetti, P. Bernier, B. Dennielou, J. A. Flores, F. J. Sierro, and M. Taviani (2006), Shoreface migrations at the shelf edge and sea-level changes around the Last Glacial Maximum (Gulf of Lions, NW Mediterranean), *Mar. Geol.*, *234*, 21–42, doi:10.1016/j.margeo.2006.09.012.

Jull, M., and D. McKenzie (1996), The effects of deglaciation on mantle melting beneath Iceland, *J. Geophys. Res.*, *101*(B10), 21,815–21,828, doi:10.1029/96JB01308.

Kaban, M. K., O. G. Flóvenz, and G. Pálmason (2002), Nature of the crust-mantle transition zone and the thermal state of the upper mantle beneath Iceland from gravity modelling, *Geophys. J. Int.*, *149*, 281–299, doi:10.1046/j.1365-246X.2002.01622.x.

Kjemperud, A. (1986), Late Weichselian and Holocene shoreline displacement in the Trondheimsfjord area, central Norway, *Boreas*, *15*, 61–82.

Larsen, C. F., R. J. Motyka, J. F. Freymuekke, K. A. Echelmeyer, and E. R. Ivins (2004), Rapid uplift of southern Alaska caused by recent ice loss, *Geophys. J. Int.*, *158*, 1118–1133, doi:10.1111/j.1365-246X.2004.02356.x.

Lundin, E., and A. G. Doré (2002), Mid-Cenozoic post-breakup deformation in the passive margins bordering the Norwegian-Greenland seas, *Mar. Pet. Geol.*, *19*, 79–93.

Martinec, Z., and D. Wolf (2005), Inverting the Fennoscandian relaxation-time spectrum in terms of an axisymmetric viscosity distribution with a lithospheric root, *J. Geodyn.*, *39*, 143–163, doi:10.1016/j.jog.2004.08.007.

Menke, M., M. West, B. Brandsdóttir, and D. Sparks (1998), Compressional and shear velocity structure of the lithosphere in northern Iceland, *Bull. Seismol. Soc. Am.*, *88*, 1561–1571.

Mortensen, A. K., M. Bigler, K. Grönvold, J. P. Steffensen, and S. J. Johnsen (2005), Volcanic ash layers from Last Glacial Termination in the NGRIP ice core, *J. Quat. Sci.*, *20*, 209–219, doi:10.1002/jqs.908.

Norddahl, H. (1990), Late Weichselian and early Holocene deglaciation history of Iceland, *Jokull*, *40*, 27–48.

Norddahl, H. (1991), A review of the glaciation maximum concept and the deglaciation of Eyjafjörður, north Iceland, in *Environmental Change in Iceland: Past and Present*, edited by J. L. Maizels and C. J. Caseldine, pp. 31–47, Kluwer Acad., Dordrecht, Netherlands.

Norddahl, H., and H. Halfidason (1992), The Skogar tephra, a Younger Dryas marker in north Iceland, *Boreas*, *21*, 23–41.

Norddahl, H., and H. G. Pétursson (2005), Relative sea-level changes in Iceland: new aspects of the Weichselian deglaciation of Iceland, in *Iceland: Modern Processes and Past Environnements*, edited by C. Caseldine et al., pp. 25–78, Elsevier, Amsterdam.

Pagli, C., F. Sigmundsson, B. Lund, H. Geirsson, E. Sturkell, P. Einarsson, and T. Árnadóttir (2006), Ongoing and future glacio-isostatic crustal adjustments around Vatnajökull ice cap, Iceland, due to ice retreat: GPS measurements and finite element modeling, *Geophys. Res. Abstr.*, *8*, 06726.

Peltier, W. R. (1974), The impulse response of a Maxwell Earth, *Rev. Geophys.*, *12*, 649–669.

Peltier, W. R. (2005), On hemispheric origins of meltwater pulse 1a, *Quat. Sci. Rev.*, *24*, 1655–1671, doi:10.1016/j.quascirev.2004.06.023.

Peltier, W. R., and R. G. Fairbanks (2006), Global glacial ice volume and Last Glacial Maximum duration from an extended Barbados sea level record, *Quat. Sci. Rev.*, *25*, 3322–3337.

Saemundsson, K. (1978), Fissure swarms and central volcanoes of the neovolcanic zones of Iceland, *Geol. J.*, *10*, special issue, 415–432.

Saemundsson, K. (1979), Outline of the geology of Iceland, *Jokull*, *29*, 7–28.

Sheth, H. C. (1999), Flood basalts and large igneous provinces from deep mantle plumes: Fact, fiction, and fallacy, *Tectonophysics*, *311*, 1–29, doi:10.1016/S0040-1951(99)00150-X.

Sigmundsson, F. (1991), Post-glacial rebound and asthenosphere viscosity in Iceland, *Geophys. Res. Lett.*, *18*(6), 1131–1134, doi:10.1029/91GL01342.

Sjöberg, L., M. Pan, S. Erlingsson, E. Asenjo, and K. Árnason (2004), Land uplift near Vatnajökull, Iceland, as observed by GPS in 1992, 1996, and 1999, *Geophys. J. Int.*, *159*, 943–948, doi:10.1111/j.1365-246X.2004.02353.x.

Stewart, I. S., J. Sauber, and J. Rose (2000), Glacio-seismotectonics: Ice sheets, crustal deformation and seismicity, *Quat. Sci. Rev.*, *19*, 1367–1389, doi:10.1016/S0277-3791(00)00094-9.

Thoma, M., and D. Wolf (2001), Inverting land uplift near Vatnajökull, Iceland, in terms of lithosphere thickness and viscosity stratification, in *Gravity, Geoid and Geodynamics 2000*, edited by M. G. Sideris, pp. 97–102, Springer, Berlin.

Thordarson, T., and A. Hoskuldsson (2002), *Classic Geology in Europe*, vol. 3, *Iceland*, 200 pp., Terra, Harpenden, U.K.

Turcotte, D. L., and G. Schubert (2002), *Geodynamics*, 2nd ed., 455 p., Cambridge Univ. Press, New York.

Van Vliet-Lanoë, B. (2005), *La planète des glaces: histoire et environnements de notre ère glaciaire*, Vuibert, Paris.

Van Vliet-Lanoë, B., A.-S. Van Cauwenberge, O. Bourgeois, O. Dauteuil, and J.-L. Schneider (2001), A candidate for the Last Interglacial record in northern Iceland: The Sydra formation. Stratigraphy and sedimentology, *C. R. Acad. Sci. Ser. IIa*, *332*, 577–584.

Van Vliet-Lanoë, B., A. Gudmundsson, H. Guillou, R. A. Duncan, D. Genty, G. Ben Gassem, S. Gouy, P. Récourt, and S. Scaillet (2007), Limited glaciation and very early deglaciation in central Iceland: Implications for climate change, *C. R. Geosci.*, *339*, 1–12.

Watts, A. B. (2001), *Isostasy and Flexure of the Lithosphere*, 458 pp., Cambridge Univ. Press, New York.

Zhong, S., and A. B. Watts (2002), Constrains on the dynamics of mantle plumes from uplift of the Hawaiian Islands, *Earth Planet. Sci. Lett.*, *203*, 105–116, doi:10.1016/S0012-821X(02)00845-2.

Zobin, V. M. (1999), The fault nature of the Ms 5.4 volcanic earthquake preceding the 1996 subglacial eruption of Grimsvötn volcano, Iceland, *J. Volcanol. Geotherm. Res.*, *92*, 349–352, doi:10.1016/S0377-0273(99)00060-8.

G. Biessy and O. Dauteuil, Géosciences Rennes, UMR 6118 CNRS, Université de Rennes 1, Campus Beaulieu, bât. 15, F-35042 Rennes CEDEX, France. (guillaume.biessy@univ-rennes1.fr)

B. Van Vliet-Lanoë and A. Wayolle, Processus et Bilan des Domaines Sédimentaires, UMR 8110 CNRS, Université de Lille 1, F-59655 Villeneuve d'Ascq, France.